Chapter 5 Manganese Crusts

5-1 Classification and Layered Structure of Manganese Crusts

In this report, manganese crusts are classified by their shape into crust, cobble crust, and nodules. The section of the crust is divided into the outer, inner and innermost layers. Photographs of typical crusts are shown in Figure 5-1-1.

(1) Classification of manganese crusts

Manganese crusts of the survey area are classified into the following three types by the shape of the crust and the host rock. Also when the manganese crust is very thin, " coating " or " sooty " will be prefixed to the classified name. Coating will be used when manganese oxide less than 1 mm thick covers the entire substrate and is black in color. Sooty will be used when only a minute amount of manganese oxide is attached to the rock and the color is dark brown to brown.

① Crusts (Fig. 5-1-1, Photo A, B)

Crust is a material whose upper surface and the sides are covered by manganese oxide and the substrate is exposed on the bottom surface. Manganese crusts are divided into 1 ∼ 3 layers and the thicker ones tend to consist of many layers.

There are two modes of occurrences of manganese crusts; one forms directly on the substrate and the other on the surface of secondary sediments. Thick manganese crusts often form botryoidal structure (Fig. 5-1-1, Photo A, B). The substrates are mostly basalt, basaltic pyroclastic rocks, and limestone. Substrates were not collected in the sample shown in Photograph B.

② Cobble crusts (Fig. 5-1-1, Photos C ∼ F)

Cobble crust is a cobble-shaped material whose entire surface is covered by manganese oxides with nucleus consisting of rock fragments and other material. The long axis of the cobble exceeds 8 cm.

These are formed by manganese crusts covering lava fragments, rock pebbles, talus deposits, boulders, and other material separated from the bedrock. Generally, the upper surface is covered by crusts thicker than the bottom, and the upper surface is botryoidal while the bottom surfaces have granular structure. Those with thick crusts are often ellipsoidal. The substrates are mostly basaltic pyroclastic rocks, conglomerate, and limestone.

A

Crust upper surface: botryoidal (MC10CB06)

B

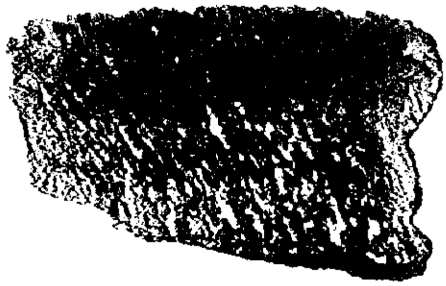

The same as the left section: lower cavities are filled with ooze

C

Cobble crust upper surface: granular (MC10CB07)

D

The same as the left bottom surface: granular

E

The same as the above section: three layers substrate rock is hyaloclastite

F

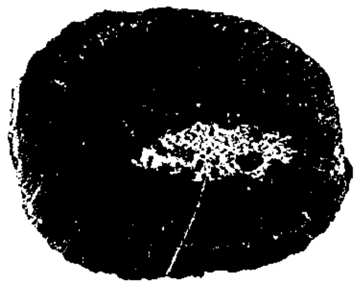

Cobble crust section: three layers (MC08CB05) substrate rock is hyaloclastite

G

Nodule upper surface: botryoidal (MC10CB19)

H

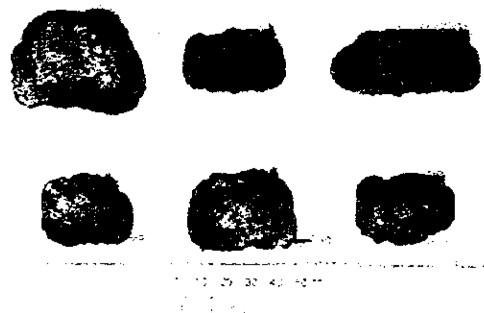

The same as the left section: one layer

Fig. 5-1-1 Photographs of manganese crusts

③ Nodules (Fig. 5-1-1, Photos G, H)

Nodule is a material smaller than 8 cm in diameter and is covered entirely by manganese oxide. Since nodules are small, they generally are mono-layered, but multi-layered nodules similar to cobbles are sometimes found although rarely.

Nodules are formed under conditions similar to cobble crust, namely manganese crust covering small rock fragments separated from the bedrock. They often lack nucleus of rock fragments (Fig. 5-1-1, Photo H upper row center). They have spherical, flat, platy, and irregular forms. The surfaces are most often botryoidal, but the structure varies with the thickness of the crust and the shape of the nodule. The nuclei material varies widely and they are; basalt, basaltic pyroclastic rocks, sandstone, mudstone, limestone, phosphorite, manganese crust fragments, foraminifera sand and others.

(2) Layered structure of manganese crusts

When manganese crusts attain certain thickness, they are divided into many layers. Generally, they are divided into two, namely the outer and inner layers (Fig. 5-1-1, Photo B), but often another layer exists at the innermost side and thus is divided into three layers (Fig. 5-1-1, Photo F). Each layer reflects the age, environment, growth rate, and other relevant factors pertaining to the formation of that particular layer. In the present study, the crusts are divided into three layers (outer, inner, and innermost) and chemical analysis, various tests, and statistical analysis of each layer have been carried out. The characteristics of each layer observable by the unaided eyes are as follows.

① Outer layer

This is the surface manganese crust layer and it often has botryoidal ~ granular surface. Its section is rather compact and its fractured surfaces is lustrous, also at times it is porous and includes brown iron oxide contamination. In thin manganese crusts, inner and innermost layers are lacking and this layer directly covers the substrate rocks.

The upper part not accompanied by pale brown filling are shown in Photo B of Figure 5-1-1, Photograph H corresponds to the whole part covering the rock fragment core.

② Inner layer

This is the manganese crust on the inner side of the outer layer. It directly covers the substrate rock when the innermost layer is missing. The fractured surface is somewhat rough and contains pores parallel to the direction of the growth of the crust, these pores often contain unconsolidated muddy material. Brown iron contamination occurs at the boundary with the outer layer. The section of the outer surface of this inner layer sometimes has botryoidal structure. The boundary with the innermost layer is very porous and is often contaminated by mud and brown iron oxides.

The lower part filled by pale brown soft mud is shown in Photograph B, and the pale brown ellipsoidal part between the outer two layers is shown in Photograph F.

③ Innermost layer

This occurs on the inner side of the inner layer and directly covers the substrate. This layer is often missing. The structure of the section is very compact and hard and the fractured surface is lustrous. The parts near the substrate rock at times is accompanied by pale brown ~ white phosphorite network, and this is phosphatized soft mud which filled the voids. On the other hand, the parts without impurities have very thin banded structure. The boundaries with the inner layer on the outerside often show irregular section. At times they are unconformable.

The part shown in Photograph E corresponds to the somewhat brown layer immediately over the grayish brown substrate rock on the lower side and the black chevron layer over the white phosphorite which overlies the brown innermost part.

5-2 Results of FDC Observation

TV-mounted deep sea towing system (FDC) was used for clarifying the mode of occurrence of the manganese crusts of the seamounts. The FDC track lines were designed to transect the high MBES acoustic pressure zones (where the manganese crusts occur). In other words, the track lines were set from the summits or from their peripheries along the steepest slope of the seamounts. The direction of towing was limited to northwestward ~ westward ~ southwestward by the current and the wind direction, and thus the track lines are mostly on the northwest ~ southwestern slope of the seamounts. Observation was carried out over a total of nine track lines, namely 1 ~ 2 lines for each of the six areas; MC03, MC04, MC07 ~ MC10.

Representative FDC seafloor photographs are shown in Figures 5-2-1 (1), (2), FDC survey results in Appendix Table 1, FDC route maps (plans and sections) and maps showing the crust exposure ratios are laid out in Apeendix Figures 4 (1) ~ (9).

The results of the TV observation of each seamount are reported below. The manganese crusts are described in accordance with the classification reported earlier. The crust exposure ratio is the areal extent of the manganese crust exposures (crusts, cobble crusts, nodules) without unconsolidated cover on the seafloor expressed in percentage of the area surveyed, and it is shown in an average value during one minute observation. The width of the seafloor sweep by TV camera is about 3 m.

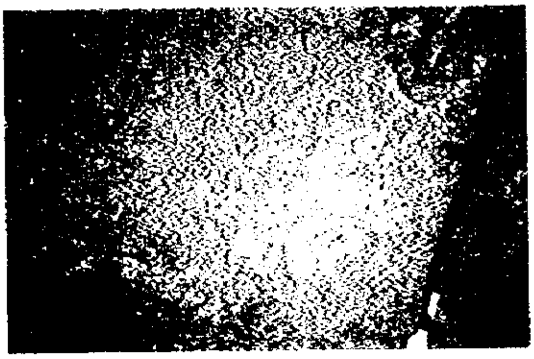

97SMC07FDC01
Crust
Pinnacle on flat summit Water depth: 1,569m
6° 01.590´N 157° 25.459´E

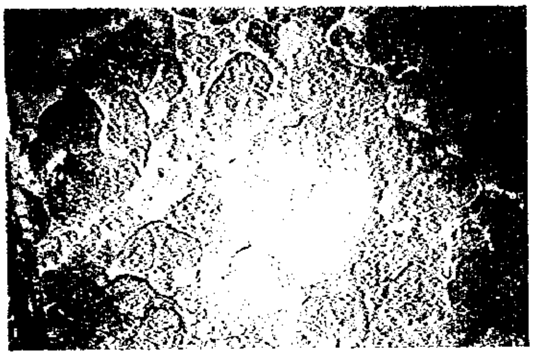

97SMC10FDC01
Crust, rough surface like lump
Upper flank Water depth: 2,110m
9° 55.558´N 148° 12.971´E

97SMC08FDC01
Crust
Flat summit margin Water depth: 2,084m
10° 21.929´N 156° 44.861´E

97SMC10FDC01
Cobble crust, talus gravels
Middle flank Water depth: 2,319m
9° 56.106´N 148° 11.275´E

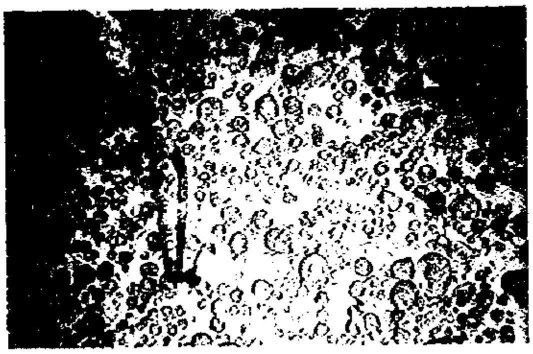

97SMC08FDC02
Cobble crust and nodule
Pinnacle on flat summit Water depth: 2,111m
10° 26.129´N 156° 40.416´E

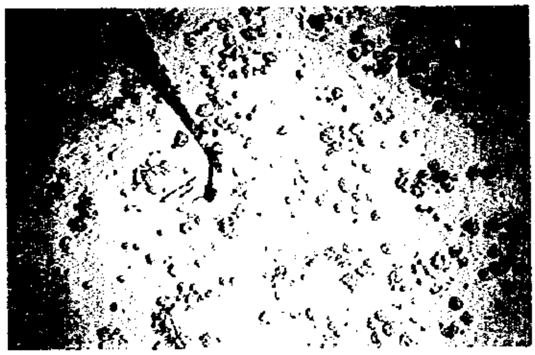

97SMC08FDC01
Nodule
Flat summit margin Water depth: 2,143m
10° 22.174´N 156° 45.058´E

Fig. 5-2-1 (1) Photographs of FDC seafloor observation

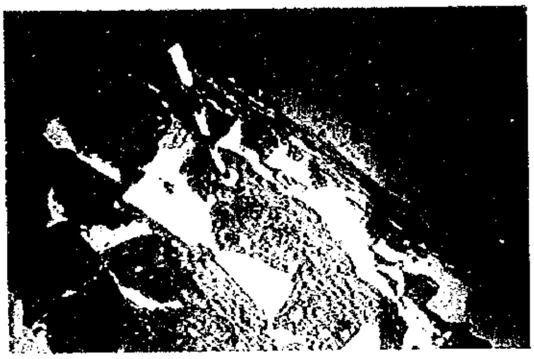

97SMC03FDC011
Cliff and crust
Lower flank　Water depth: 2,801m
6° 19.537′N　141° 29.252′E

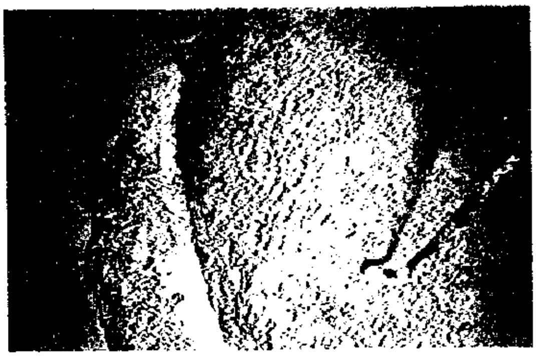

97SMC07FDC01
Step-like outcrop of crust
Upper flank　Water depth: 2,028m
6° 02.385′N　157° 22.880′E

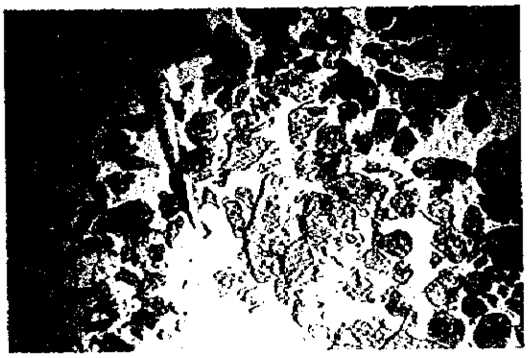

97SMC03FDC010
Mn-coating gravels of limestone
Summit　Water depth: 1,084m
6° 17.872′N　141° 32.187′E

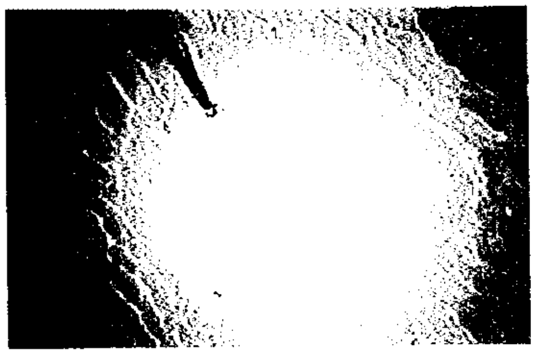

97SMC10FDC01
Foraminiferal sand and ripple mark
Flat summit margin　Water depth: 2,205m
9° 55.610′N　148° 12.608′E

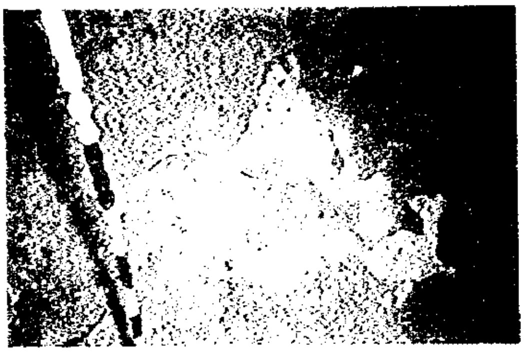

97SMC04FDC02
Limestone
Summit　Water depth: 220m
6° 15.345′N　114° 20.909′E

97SMC08FDC01
Hyaloclastite
Middle flank　Water depth: 2,634m
10° 22.719′N　156° 45.469′E

Fig. 5-2-1 (2) Photographs of FDC seafloor observation

(1) MC03 area

1) Track line 97SMC03FDC010

This track line is located on the northwestern slope of the of the western part of the seamount, extending from the summit (980 m deep) to the middle slope (2,751 m). The direction of the track line (observation) is northwest to 2,300 mn of water depth then northeast for the deeper parts with a inverted L-- shape. The total length of the observation is 3.8 miles.

The summit has many steep cliffs, the upper and the middle slope also have cliffs and steps of about 5 m displacement. The gradient of the upper slope above 1,500 m water depth and the middle slope around 2,500 m depth is steep with gentle gradient in between.

Crusts occur dominantly on the summit, around 11,500 m water depth on the lower apart of the summit, around 2,100 m depth on the upper slope, at 2,350 ~ 22,750 m depth on the middle slope. The exposure ratio is approximately 90 %, 50 %, 70 %, and 40 % respectively. The cobble crusts occur extensively immediately below the summit at around 1,100 m depth and on the upper slope around 1,950 m depth. The exposure ratio is 70 % and 60 % respectively., The foraminifera sand cover tends to increase and the crust exposure ratio decrease with the increase of water depth. In areas other than the above, the crust exposure ratio is low at 0 ~ 10 % because of the entire coverage by foraminifera sand, or partial exposure of crust and scattered occurrence of cobble crusts because of the thick sand. The surface of the manganese crusts are granular to flat.

Nodules occur only locally in the depressions of the summit, and are not observed in other localities. In these depressions the nodules and cobble crusts occur on foraminifera sand thinly covering the crusts.

Foraminifera sands are predominant in the gentle slope at 1,550 ~ 2,050 m and 2,250 ~ 2,350 m depths. The exposure ratio of the crusts here is mostly 0 % the very locally around 10 %. There are ripple marks throughout the surface of the foraminifera sands.

The many cobble crusts observed at 1,100 m depth immediately below the summit is very similar to those collected from the summit of the seamount to the south MC03CB06. These crusts coat the substrate in around 1 mm thickens and thus those observed above 1,500 m depth are believed to be also similarly thin.

2) Track line 97SMC033FDC011

This track line is located on the northern slope in the western part of the seamount, and extends from the middle slope (2,640 m deep) to the lower slope (3,870 m deep). The direction of the line is northwest and the observed length is 1.9 miles.

The slope is steep at 2,750 ~ 3,100 m depth and 3,350 ~ 3,500 m depth, and the gradient is gentle in other places with steep cliffs and step-wise cliffs in some places.

The crusts are exposed dominantly in the steep slopes with 30 ~ 80 % exposure ratio. In areas other than the above, crusts and cobble crusts are exposed only partially with an exposure ratio of around 10 % or 0 %. The slope is the most gentle within this track line at 3,250 ~ 3,350 m depth (10°) and here the foraminifera sand is predominant with hardly any crust exposures with ratio of 0 %.

Generally the foraminifera sands are thickly deposited, and the manganese crusts are exposed intermittently, often with the marginal parts of the crust exposed partially. The surface of the manganese crusts is granular to smooth. Nodules were almost non-existent in this track. Ripple marks occur throughout the foraminifera sands.

(2) MC04 area

1) Track line 97SMC04FDC01

The track line is located on the southwestern slope of the western part of the summit and extends from the upper slope (1,860 m depth) to the lower slope (3,636 m depth). The direction of the line is southwest and the observed length is 3.8 miles.

The slope is very steep at 2,200 ~ 2,650 m and 3,100 ~ 3,400 m depths, gradient is gentle at other depths. Steep cliffs with 5 ~ 10 m displacement occur in the steep parts and at the ridge in the northeastern edge of this track line.

Crusts are dominant at the gentle middle slope with 2,050 ~ 2,200 m depth and 2,400 ~ 2,650 m depth below the steep slope, and the exposure ratio is 40 ~ 100 % and 10 ~ 40 % respectively. The depth between the above, 2,200 ~ 2,400 m, is steep slope and foraminifera sands are predominant with crust exposure ratio of 0 ~ 10 %. Also the crust exposure ratio is low at 10 ~ 20 % at the steep lower slope of 3,100 ~ 3,350 m depth. In other areas of this track line, the crust occurs sporadically as cobbles on foraminifera sand or the edge of the crust peeks out through thick foraminifera sands and the continuity is poor with exposure ratio of 5 ~ 10 %.

Nodules have not been observed by this line. Ripple marks and traces occur throughout the foraminifera sands.

Only coating of manganese crust (reef limestone substrate) with less than 1 mm thickness was collected at 97SMC04CB05 sampled at the upper slope at the northeastern edge of this track line. The surface of the manganese crusts observed along this track line are granular to smooth and botryoidal structure were not observed. Thus it is inferred that the manganese crusts here are thin.

2) Track line 97SMC04FD02

The track line is located on the southwestern slope of the western seamount and extends from the summit (220 m depth) to the middle slope (2,600 m depth). The direction of the line is southwest and the observed length is 5.0 miles.

The topography consists of four steep parts of the slope, one flat terrace, one depression, and other gentle parts of the slope. The terrace is at 800 ~ 900 m depth, the depression where the track line crossed the valley at about 1,300 m depth.

White limestone (eroded holes observed) without manganese crust cover is exposed from the summit to the upper slope (800 m depth). Foraminifera sand is almost non existent on the summit, and at the base of the slope (700 ~ 850 m depth) limestone talus pebbles are scattered with foraminifera sand deposited among them.

Manganese crusts were observed at the central part of the terrace deeper than 850 m. Crusts are predominant at the step parts, but the exposure is intermittent and the exposure ratio is extremely variable at 10 ~ 90 % and the average is 30 ~ 40 %. Cobble crust occurs on the foraminifera sand and is exposed intermittently at the terrace and the valley with exposure ratio of 50 ~ 100 % and around 10 % respectively.

The surface of the crusts is smooth and botryoidal structure is not observed. Nodules have not been observed. Ripple marks are not common on the surface of the foraminifera sands.

(3) MC07 area

1) Track line 97SMC07FDC01

The track line is located on the western slope of the seamount extending from the central part of the summit (1,550 m depth) across the flat summit to the middle slope (2,940 m depth). The direction of the line is west– northwest and the observed distance is 6.3 miles.

There are many small hills with relative height of several hundred meters from the flat summit to the upper slope. The eastern end of the track line is located at the summit of a small hill, and the central part of the line transects the foot of two small hills. Aside from these two localities the gradient is very gentle above 2,250 m, becoming somewhat steeper at 22,450 ~ 2,800 m depth.

Crusts are dominant at; 1,550 ~ 1,870 m depth on the summit of a small hill, 1,980 ~ 2,050 m depth on the periphery of the flat summit, and 2,100 ~ 2,300 m depth on the upper slope. The crust exposure ratio of these parts is; 50 ~ 100 %, 40 ~ 100 %, and 20 ~ 90 % respectively. It is seen that the exposure ratio decreases and the continuity deteriorates with the water depth. Cobble crusts and nodules occur immediately above the crust at the foot of the small hills. The cobble crusts are angular to subrounded with major axis ranging from 20 to 50 cm, while the nodules are spherical with diameter ranging from 5 to 10 cm. The crusts are locally and intermittently exposed at; 2,400 ~ 2,800 m depth on the middle slope with exposure ratio of 0 ~ 80 %.

The crust surface is botryoidal on the summit and upper slope, while it is smooth on the middle slope. Manganese crust samples collected at 97SMC07AD07 consist of only thin coating (under 1 mm thick) on parts of basalt fragments.

Manganese crusts occur only near small hills above 2,100 m depth, and other areas are dominantly covered by foraminifera sands. Ripple marks occur throughout the surface of the foraminifera sands, and marks generally show parallel wave form, but in some localities, they locally cross each other at right angles or radiate in various directions.

(4) MC08 area

1) Track line 97SMC08DC01

The track line is located at the eastern part of the seamount, and it extends from the margin (2,040 m depth) of the summit to the middle slope (3,250 m depth). The direction of the line is northeast and the length of observation is 2.4 miles.

The gradient of the summit periphery is very gentle, and the upper to the middle slope is very smooth without notable relief. The upper slope is actually very steep, but the topographic section prepared has an apparent gentle slope because the track line runs oblique to the direction of the maximum gradient.

Crusts are continuously exposed from the summit periphery of 2,060 m depth to the middle slope 3,150 m deep. The exposure ratio exceeds 40 % at; ridge of the upper slope at 2,450 ~ 222,650 m depth and middle slope around 3,150 m depth. The other three localities are the steeper parts of the slope. Cobble crusts generally occur scattered, and tend to be dominant at gentle slope. Nodules occur at the summit periphery and middle slope deeper than 3,000 m.

The surface of the crusts is botryoidal at the periphery of the flat summit, smooth to granular at the middle slope. Bedrock (probably hyaloclastite) without manganese crust cover was observed at 2,420 m and 2640 m depths.

Foraminifera sands are dominant at; most of the summit periphery, from 2,750 m to 2,950 m depth, and below 3,150 m, and the crust exposure ratio is 0 ~ 10%. Ripple marks occur on the foraminifera sand surface throughout the track line.

2) Track line 97SMC08FDC02

The track line is located at the northwestern part of the summit, and it extends from the tope of a small hill (1,850 m depth) down its northern slope to the edge of the summit (2,300 m depth). The direction of the line is north–northeast and the observed length is 2.1 miles.

This small hill is shown with a conical shape in the topographic map, and the relative height is 250 m. The summit is almost flat without relief except this small hill.

Crusts are continuously exposed on this small hill and its foot area (around 2,140 m depth), and there are cobble crusts and nodules in some parts. The exposure ratio is high at 50 ~ 90 % with an average of 50 %. On the other hand, the periphery of the summit is dominated by foraminifera sands and the crusts are covered with intermittent outcrops and the exposure ratio is 10 ~ 70 % with an average of 15 %. There are three significant localities on this summit where the exposure ratio exceeds 40 %, and these are inferred to be parts with steep gradient.

The surface of the crusts are botryoidal or smooth. Cobble crusts occur on the slopes of the small hill, and nodules at the foot of this hill. Ripple marks occur throughout the surface of the foraminifera sands.

Crusts (70 mm maximum thickness, average 30 mm) with granular surface were collected at 97SMC08CB14 on the southern slope of the small hill. Also crusts and nodules (25 mm maximum thickness, average 10 mm) with botryoidal to granular surface, and coated cobbles (average less than 1 mm thick) were collected at 97SMC08CB04 on the summit periphery near 2,150 m depth. These results of sampling is harmonious with the results of observation.

(5) MC09 area

1) Track line 97SMC09FDC01

The track line is located on the southern slope of the southern seamount and extends from the summit (1,100 m depth) to the middle slope (2,850 m depth). The direction of the line is southwest and the observed length is 2.3 miles.

The slope is, on the whole, steep but the track line crosses a valley in the central part and the topographic section shows a depression. The slope is full of small undulations throughout and steep and linear cliffs are developed.

Crusts and cobble crust are continuously exposed from the summit to the valley in the central part of the track line (1,100 ~ 2,150 m depth). The exposure ratio is 20 ~ 100 % with high average of 60 %. The slope to the west of the valley (deeper than 2.150 m) is dominated by foraminifera sand and the crusts are intermittently exposed with ratio decreasing to 5 ~ 40 %. In the valley (2,150 ~ 2,200 m depth), the foraminifera sand is thick and the crusts are exposed only locally.

The surface of the crusts are generally granular to smooth with relatively few botryoidal structure. The cobble crusts are distributed under cliffs and in depressions and they are angular with 20 ~ 40 cm long axis. Nodules are rare and they occur on the foraminifera sands of the valleys and gentle middle slopes. Ripple marks occur throughout the foraminifera sands.

(6) MC10 area

1) Track line 97SMC10FDC01

The track line is located on the northwestern slope of the seamount. It extends from the periphery of the flat summit (1,950 m depth) to the lower slope (3,550 m depth). The direction of the line is west–northwest and the observed length is 4.8 miles.

The summit and the upper slope to 2,400 m depth have flat to very gentle gradient. Terraces are formed between 2,300 and 2,400 m depth. The gradient of the middle to the lower slope below 2,400 m depth is steep and becomes somewhat gentle below 2,800 m depth.

Crusts and cobble crusts are exposed continuously on the slope above the terraces on the upper slope (1,200 ~ 2,200 m depth) and from the shoulders of the terraces to the middle slope (2,350 ~ 2,800 m depth). The exposure ratio is 40 ~ 90 % (average 65 %) and 40 ~ 100 % (average 80 %) respectively. Crusts and cobble crusts are exposed intermittently at the eastern end of the track line at the periphery of the summit and on the lower slope below 2,900 m depth. The exposure ratio is 20 ~ 100 % and 10 ~ 40 % respectively. Crusts are dominant in the gentle slope above 2,400 m depth, while cobble crusts are dominant on the steep slope below the above depth. The crusts take; lumpy, cemented cobbles, pavement, and other forms, and the surface is botryoidal or flat. The cobble crusts are subrounded with 30 ~ 60 cm diameter, and boulders exceeding 1 m diameter are not uncommon. Angular talus cobbles occur at the foot of the very steep slope near 2,750 m depth.

Nodules occur locally at the periphery of the summit margin and the shoulder of the terraces, as well as at the gentle middle to lower slope mixed with cobble crusts.

Foraminifera sands are thickly deposited on the terraces at 2,200 ~ 2350 m depth and manganese crusts are not exposed. Foraminifera sands are also predominant on the lower slope below 2,800 m depth covering manganese crusts. Ripple marks occur throughout the surface of the foraminifera sands.

Crusts with botryoidal surface (maximum thickness 107 mm, average 90 mm thick) were collected to the north of the eastern edge of this track line in the upper slope above the terraces by 97SMC10CB06.

5–3 Results of Sampling

Manganese crusts were sampled at MC02～MC10 areas by dredges (CB, AD) or corer (LC). The sampling points were selected where the MBES image showed high acoustic pressure (manganese crusts are exposed on the seafloor). These points were designed to cover the entire seamount from the summit to the lower slope with homogeneous density. Some of the sampling points were selected from seafloor observation by FDC. The total number of sampling points was 128 points in nine areas; 104 dredge points and 24 corer points. Crusts in quantities sufficient for chemical analysis could not be collected at 39 dredge points and 20 corer points, a total of 59 points.

The following is the description of the collected samples from each locality. The localities are shown in Figures 4–2–1 (1)～(9), the summary of collected materials are listed in Appendix Tables 2 (1)～(7), and the summary of the sampling results in Table 5–3–1. Photographs of representative dredged manganese crusts are shown in Figure 5–1–1.

1) MC02 area

The average thickness of the manganese crusts here is 21 mm with a maximum of 50 mm. This average thickness is the largest in the whole nine areas surveyed, but it should be noted that the number of sampling points is only four. Of this four points 2～5 cm thick crusts were collected at three points on the summit. The remaining one point is located at the lowermost part of the slope and sooty manganese oxide is attached to parts of metabasalt substrate. There are no data regarding the middle～upper slope, but it is inferred from the results of other areas that manganese crusts with several centimeter thickness occur there.

Crust sample with maximum thickness was collected by MC022CB04 on a small hill in the southwestern part of the summit. This crust is divided into two layers and the inner layer is 20～35 mm thick. A section of the inner layer shows notable linear parallel voids filled by soft mud (similar to Fig. 5–1–1, Photo B). These linear voids indicate the direction of the growth of the manganese crusts and it is not normal to the substrate surface, but at 60～80° angle.

2) MC03 area

The average thickness of the manganese crusts is 8 mm with maximum of 47 mm. There are five sampling points out of 12 where the average manganese crust thickness exceeds 10 mm. The thickness tends to increase at the eastern part of seamounts with flat parts. Thin cobble crusts and manganese oxide coatings were collected in this area at shallow summits and small hills, and 10～20

Table 5-3-1 Summary results of sampling

District	No. of sampling site	No. of site crust collected	Water depth of site crust collected (m)		Crust thickness (mm)		Average ore grade (%)						Geology (K-Ar age of basalt)		
			Max	Min	Max	Min	Co	Ni	Cu	Fe	Mn	n	Summit	Upper flank	Lower flank
MC02	7	4	3,335	1,482	50	21	0.35	0.33	0.08	17.44	19.67	4	Limestone	Basalt	Basalt (22Ma)
MC03	16	12	2,907	1,177	47	8	0.48	0.36	0.05	15.95	24.21	16	Limestone	Limestone Basalt (12.5Ma)	Basalt
MC04	21	17	2,651	485	20	1	0.47	0.32	0.03	14.46	27.13	7	Limestone	Limestone Basalt	Basalt (11.4Ma, 14Ma)
MC05	9	7	3,048	1,417	< 1	< 1	-	-	-	-	-	0	Limestone	Limestone	Basalt (10.8Ma)
MC06	8	8	2,636	1,625	20	3	0.47	0.36	0.04	16.25	24.88	8	Limestone	Limestone	Basalt
MC07	15	10	2,941	1,671	14	5	0.48	0.31	0.04	15.16	26.15	7	Limestone Basalt (6.4Ma)	Basalt (0.92Ma)	Basalt
MC08	19	18	5,208	1,836	90	20	0.36	0.32	0.09	15.96	23.67	32	Basalt (46.5Ma) Mudstone	Basalt (25.0Ma)	Basalt
MC09	13	13	4,758	1,370	23	7	0.49	0.30	0.05	15.62	25.57	16	Basalt (11.0Ma)	Basalt (5.2Ma)	Basalt
MC10	20	16	2,810	1,741	155	20	0.33	0.30	0.07	22.67	15.92	23	Basalt, Mudstone (69.0, 24.0Ma)	Basalt	Basalt

mm thick crusts were collected in other parts of the seamount. Manganese crusts with reef limestone substrates tend to be thin.

Crust sample with the maximum thickness was collected by MC03CB11 in the southeastern flat area in the eastern part of the seamount. This crust is divided into two layers and the inner layer is 20 ~ 35 mm thick, and is very porous polluted by brown iron oxide. Sample was not collected at MC03LC 16 on the upper slope on the western side of the seamount, but cobble crusts were confirmed by seafloor photography.

3) MC04 area

There are two seamounts in this area, the eastern and the western. Within the whole area, the average thickness of the manganese crusts is 1 mm and the maximum 20 mm. Manganese crusts were collected at 17 sampling points, but the thickness exceeds 10 mm at only two points.

At the western seamount, the average thickness is 1 mm and the maximum 15 mm. At 10 sampling points out of ten where manganese crusts were collected, the crusts occur as coatings or sooty with average of less than 1 mm in thickness in all sampling points. Major part of the collected rocks are reef limestone and when this limestone are the substrate the crust are less than 1 mm thick. Basalt substrates have thicker manganese crust over them, but the thickness is around 1 mm. Five to 15 mm thick crusts were collected only from one locality, MC04CB17, at the upper slope of the ridge extending westward of the seamount.

At the eastern seamount, the average thickness is 2 mm and the maximum 20 mm. The local average thickness is less than 1 mm at two of the six points where manganese crusts were collected. Most of the collected crusts were less than 5 mm thick and many of them are cobble coatings of less than 1 mm. The collected samples consists of mixtures of crusts, cobble crusts, coatings to sooty material. This is different from the western seamount where the crusts exceed 1 mm thickness on limestone substrates. Thickest crust was collected at MC04CB13 on the middle northwestern slope. This crust has botryoidal surface and is not accompanied by substrate rocks. Angular to rounded nodules with botryoidal to smooth surface were collected at MC04CB10 from the flat summit. The core of the nodules is limestone and the average thickness is 2 mm.

4) MC05 area

The average thickness of the manganese crusts is less than 1 mm and the maximum is also less than 1 mm. Manganese crusts were collected at seven sampling points, but they are all sooty to coating type oxides. Therefore, the samples from this area were not chemically analyzed.

The water depth of the summit of this seamount is only 20 m and this is the shallowest seamount if the nine areas surveyed. The sampling points are widely spread from the 3,000 m deep lower slope to the 1,400 m deep upper slope, and the collected samples vary widely such as; basalt, basaltic pyroclastic rocks, conglomerate, sandstone, and limestone, but only a very small amount of manganese crusts are attached. The manganese crusts are extremely thin, and the reason for the poor growth of the crusts is considered to be as follows. The seamount is quite young, and there has not been sufficient time for the growth of the manganese crusts. The summit was above water until recent times and clastic material were supplied to the slopes and it hindered the growth of the crusts.

5) MC06 area

The average thickness of the manganese crusts is 3 mm and the maximum 20 mm. Of the eight sampling points, the average thickness of the samples is less than 1 mm at three points and there is no sampling point where the average thickness of the collected samples exceeds 10 mm. The thickness is around 3 ~ 5 mm with hyaloclastite and limestone substrate. On the other hand, 10 mm thick crusts were collected as fragments without substrate rocks.

The thickest crust was collected in MC06CB04 near the middle northwest slope on the western peak of the seamount. This crust has granular surface and is not accompanied by substrates. Nodules with botryoidal ~ granular surface were collected in MC06CB06 from the terrace type flat part in the central peak of the seamount. The substrates for the nodules are hyaloclastite and limestone, and the crust thickness is 1 ~ 10 mm with 4 mm average.

6) MC07 area

The average thickness of the manganese crusts is 5 mm and the maximum 14 mm. Of the 10 sampling points where manganese crusts were collected, the local average thickness was 1 mm at one point, and there were no sampling points where the thickness averaged more than 10 mm. Generally only small amount of samples could be collected from the sampling points, and the major part of the collected crust samples have botryoidal ~ granular surface. The crusts are thin on the whole and none of the collected material had two layered sections.

A crust with the maximum thickness was collected at the middle eastern slope in MC07CB02. Many nodules with botryoidal to granular surface were collected in MC07CB15 in the southeastern edge of the flat summit. The hosts of the nodules are subrounded to subangular hyaloclastite and basalt, and the average thickness of the crust is 2 mm. Samples were not collected in MC076LC13 at the flat ridge of the southern part of the flat summit, extensively exposed crusts were confirmed by seafloor photographs.

7) MC08 area

The average thickness of the crusts is 20 mm and the maximum 90 mm. Of the 18 sampling points where manganese crusts were collected, the local average thickness exceeded 10 mm in 11 points and was under 1 mm at one point. Cobble crusts and crusts with botryoidal to granular surface are dominant and there are many nodules on the flat summit. The thickness of the manganese crusts tends to be greater on the flat summit and the upper slope than on the middle and lower slope in this seamount. Generally the manganese crust is divided into two or more layers when thicker than 3 cm, and into three layers when it exceeds 6 cm.

Cobble crust with maximum thickness was collected at a small hill of the northeastern part of the flat summit in MC08CB05. Seven cobble crusts larger than 20 cm in long axis and many smaller cobbles and nodules were collected here. These cobble crusts have botryoidal surface and is divided into three layers (Fig. 5-1-1, Photo F). There are many voids between the outer and inner layers and these are filled with soft mud, phosphorite network fills the border between the two layers.

All five dredged points on the flat summit and MC08CB08 and MC08CB19 on the slope yielded spherical to flat oblong nodules. Samples were not collected in MC08LC17, but nodules were confirmed by seafloor photographs at this point.

At 5,200 m depth on the western foot of the seamount, crusts overlying unconsolidated sediments were collected in MC08LC01. The surface of these crusts is smooth with small and gentle undulations and the thickness is 6 ~ 15 mm. The sediments immediately underlying the crusts (fine sand to mud) are phosphatized and are consolidated. This mode of occurrence of crusts are not found in other areas. It is seen from the seafloor photographs that the crusts are thinly covered by unconsolidated sediments and thus this point has low supply of sediments and this crusts probably occur locally.

Manganese crusts exceeding 6 cm in thickness were collected at four sampling points on the flat summit and upper slope. Of these localities, three yielded cobble crusts with different substrates, namely limestone, hyaloclastite, and mudstone, and crust with basalt substrate occurs at the remaining one point. The fact that a variety of rocks are covered by thick manganese crusts is inferred to indicate the older age of the seamount. From the modes of occurrence of the crusts, it is believed that the seamounts in the MC08 area is the oldest in the nine surveyed areas and those in MC05 area are the youngest.

8) MC09 area

The average thickness of the manganese crusts is 7 mm and the maximum of 23 mm. Of the 13 sampling points where manganese crusts were collected, the local average thickness is under 1 mm at one sampling point and it exceeds 10 mm at also one sampling point. Cobble crust with granular surface and crust are predominant, and the crust consists mostly of only one outer layer with rare occurrence of two-layered crusts. At almost all sampling points, the thickness of the manganese crusts is within the rage of maximum 10 ~ 15 mm, minimum 1 mm, with average value between 7 and 9 mm. It is characteristic of this area that the thickness of the crusts does not vary very much between the sampling points.

Crust with maximum thickness was collected in MC09CB06 at the middle northern slope of the southern seamount. This crust has granular surface and consists of one outer layer.

9) MC10 area

The average thickness of the manganese crusts is 20 mm and the maximum 155 mm. This maximum thickness is the largest of all nine areas surveyed, and there are three sampling points where the local maximum thickness exceeds 100 mm. Of the 16 sampling points where manganese crusts were collected, local average thickness exceeds 10 mm at three sampling points while it is under 1 mm at three points. Crusts with botryoidal to granular surface and cobble crusts are predominant, and nodules are abundant in the flat summit. The manganese crusts consist of two to three layers when their thickness exceeds 4 cm. Also with the nodules, those with cores consists of a single layer while those without cores are divided into two layers.

There are flat terraces on the upper to middle northern slope, and cobble crust with maximum thickness was collected at a small hill on this terrace in MC10CB07 (Fig. 5-1-1, Photo C ~ E). This cobble crust is 30 ~ 40 cm in diameter with granular surface and is divided into three layers. The average thickness on the upper side of the host rock is 140 mm, while the crust on the under side is 5 ~ 10 mm thick and it is clear that the manganese crust has grown notably on the upper side (Fig. 5-1-1, Photo E). On the upper side, the outer layer is 15 mm thick on average, inner layer 70 mm, and the innermost layer 55 mm. The three layers have not grown concentrically (Fig. 5-1-1, Photo F), and the inner layer disappears at the lower part of the cobble crust and the outer layer directly covers the innermost layer. Phosphorite layers derived from calcareous ooze are intercalated in the innermost layer, and calcareous conglomerate is included in the inner layer of the lower side. It is thus inferred that the lower part of this cobble crust was buried in the seafloor sediments when the innermost and inner layers grew. Cobble crusts with 10 mm diameter was also collected at this point and this has only one manganese crust layer and is 8 mm thick on average.

Spherical, flat oblong, and platy nodules were collected at the northern summit and upper slope of the seamount (Fig. 5-1-1, Photo G, H). The average length of the nodules is 4 cm and the surface is botryoidal to granular, and the average thickness is about 10 mm.

Manganese crusts the maximum thickness exceeding 100 mm were collected at three sampling points on the upper to middle slope on the northern to northwestern side of the seamount. With the exception of these three points, the local maximum thickness is very small at 35 mm. And it is inferred that the physicochemical environment of the vicinity of the above three points were favorable for the growth of manganese crusts. Actually the inner layers of MC10CB06 (Fig. 5-1-1, Photo B) and of MC10CB07 (Fig. 5-1-1, Photo E) have abundant voids in the direction of growth indicating fast growth rate. Also these thick manganese crusts began to form in fairly old time and the seamounts of the MC10 area are inferred to be old as in the case of MC08.

5-4 Chemical Composition of the Crusts and Statistical Analysis

The manganese crust samples collected from 69 sampling points in MC02 to MC04 areas and from MC06 to MC10 areas were chemically analyzed for the following 29 elements. For samples sufficiently thick to separate the layers of the crusts, analytical samples were collected from each layer. Also when different kinds of manganese crusts were collected from one sampling point, all types of crusts were analyzed. Therefore the number of samples analyzed amounted to a total of 163 from 69 sampling points. The results of the analysis are laid out in Appendix Tables 3 (1) ~ (4).

1) Analytical methods

Methods used for the elements are as follows. The samples were dried until constant weight was confirmed and then prepared for analysis.

- ICP emission spectrometry: Mn, Fe, Si, Al, Ti, Ca, P, Pt
- ICP mass spectrometry: Co, Ni, Cu, Pb, Zn, Mo, V, La, Ce, Pr, Nd, Sm, Eu, Gd, Tb, Dy, Ho, Er, Tm, Yb, Lu

2) Chemical composition

Manganese crusts are believed to have been formed by direct precipitation of manganese, iron and other various metals from sea water. And the major components are manganese and iron hydroxides and oxides. The chemical composition varies by the location of the seamount (local characteristics, latitude and longitude), water depth, horizon of the manganese crust (the age of formation and growth rate), constituent manganese oxide minerals.

Within the survey area, the analytical results of the manganese crusts vary by the seamount or sampling points. The ratio of the maximum and minimum content is; 2 ~ 3 for Mn and Fe, and 5 ~ 10 for Co, Ni, Cu. These variations are caused mainly by the layers of the crusts.

The average composition of the five major elements is; Co 0.41, Ni 0.32, Cu 0.06, Mn 24.08, Fe 15.86 (wt%). These values are not very different from the results obtained by USGS-KORDI (1992). Manganese crusts with cobalt content exceeding 0.5 wt% are sometimes called cobalt-rich manganese crust, but those in the present survey area do not belong to this category.

In the (Co+Ni) × 10-Fe-Mn triangular diagram of Figure 5-4-1, manganese crusts of the Central Pacific are plotted somewhat to the Mn side in the center of the diagram (J.R. Hein et al., 1992). The plots of the manganese crusts from the present survey area are in the lower central part of the diagram in the Mn side and dispersion is relatively small. It is of interest to note that the plots of the deep-sea manganese nodules are in an area similar to the manganese crusts in this diagram, while submarine hydrothermal manganese ores are plotted near the base line of this diagram joining Fe and Mn. The left column of Figure 5-4-1 are the plots of the bulk manganese crusts, and the plots of the composition by the crust layers are shown in the right column, crosses show the outer layer and black circles the inner layer, and the white circles the innermost layer.

3) Basic statistics

Basic statistical values were calculated for; each area, types of manganese crusts, position of the sample within the crust, and water depth of the sampling points. The results are laid out in Appendix Tables 4 (1) ~ (5). Basic statistics from the bulk analysis for each area is shown in Table 5-4-1.

The average values of the major elements by areas show the following characteristics.

- In MC02 area, crusts have the highest average Fe, Ti, Si, Al, Pt content and the lowest average Mn content within the whole eight areas. Also the difference with other areas is large.
- In MC04 area, crusts have an opposite trend to those of MC02. Namely they have the lowest average Fe, Ti, Si, Al, content and the highest average Mn content
- In MC08 area, the crusts have the highest average Cu, Ca, P content.
- In MC09 area, the crusts have the highest average Co content and the lowest average Pt content.
- In MC10 area, the crusts have the lowest average Co content.

Table 5-4-1 Basic statistics

Region	Co (%)			Ni (%)			Cu (%)			Mn (%)			Fe (%)			Pb (%)			Zn (%)			Ti (%)		
	Max.	Min.	Ave.	Max.	Min.	Ave.	Max.	Min.	Ave.	Max.	Min.	Ave.	Max.	Min.	Ave.	Max.	Min.	Ave.	Max.	Min.	Ave.	Max.	Min.	Ave.
MC02	0.66	0.20	0.40	0.40	0.26	0.34	0.13	0.03	0.06	28.22	16.35	20.76	19.68	13.91	17.30	0.07	0.01	0.03	0.08	0.05	0.06	1.48	0.71	1.20
MC03	0.85	0.24	0.48	0.49	0.21	0.35	0.14	0.02	0.05	28.60	18.12	23.96	17.87	12.57	16.10	0.08	0.01	0.05	0.12	0.04	0.07	1.38	0.59	0.88
MC04	0.64	0.31	0.47	0.46	0.22	0.32	0.05	0.02	0.03	30.48	22.85	27.13	16.54	12.18	14.46	0.12	0.05	0.07	0.06	0.04	0.05	0.91	0.68	0.76
MC06	0.61	0.35	0.46	0.60	0.21	0.38	0.07	0.03	0.04	29.07	16.66	25.55	20.96	14.34	15.98	0.12	0.01	0.07	0.06	0.05	0.06	1.47	0.69	0.81
MC07	0.74	0.25	0.48	0.43	0.23	0.31	0.05	0.03	0.04	32.99	21.38	26.15	17.20	11.07	15.16	0.12	0.04	0.07	0.07	0.05	0.06	1.22	0.85	0.97
MC08	0.80	0.09	0.34	0.48	0.13	0.32	0.18	0.03	0.09	30.26	12.64	23.23	20.88	10.47	16.09	0.15	0.01	0.07	0.09	0.05	0.06	1.32	0.58	1.01
MC09	0.93	0.25	0.48	0.41	0.13	0.30	0.06	0.02	0.05	32.27	22.68	25.38	17.14	12.47	15.52	0.12	0.03	0.08	0.06	0.03	0.05	1.06	0.68	0.90
MC10	0.57	0.09	0.31	0.45	0.13	0.28	0.16	0.03	0.07	26.58	10.35	20.99	21.53	9.90	16.07	0.15	0.03	0.08	0.10	0.04	0.06	2.48	0.49	0.99
All	0.93	0.09	0.39	0.60	0.13	0.32	0.18	0.02	0.07	32.99	10.35	23.43	21.53	9.90	15.95	0.15	0.01	0.07	0.12	0.03	0.06	2.48	0.49	0.96

Region	Mo (%)			V (%)			Si (%)			Al (%)			Ca (%)			P (%)			Pt (ppm)		
	Max.	Min.	Ave.	Max.	Min.	Ave.	Max.	Min.	Ave.	Max.	Min.	Ave.	Max.	Min.	Ave.	Max.	Min.	Ave.	Max.	Min.	Ave.
MC02	0.05	0.01	0.03	0.07	0.05	0.06	8.18	1.72	5.01	2.75	0.34	1.59	2.37	1.82	2.08	0.48	0.24	0.40	0.90	0.20	0.54
MC03	0.05	0.02	0.03	0.07	0.05	0.06	6.87	1.57	3.24	2.19	0.35	0.86	6.39	2.13	2.69	0.56	0.35	0.43	0.80	0.10	0.33
MC04	0.06	0.02	0.04	0.07	0.05	0.06	4.06	1.80	2.56	0.90	0.43	0.64	2.71	2.16	2.40	0.47	0.30	0.39	0.30	0.10	0.23
MC06	0.05	0.01	0.04	0.07	0.05	0.06	5.11	2.68	3.19	1.41	0.60	0.79	2.56	1.55	2.27	0.50	0.39	0.43	0.60	0.20	0.26
MC07	0.05	0.02	0.03	0.06	0.05	0.06	5.75	1.46	3.19	1.30	0.41	0.69	2.38	2.25	2.30	0.42	0.32	0.37	0.30	0.10	0.19
MC08	0.07	0.02	0.04	0.08	0.05	0.06	7.81	0.96	3.24	2.78	0.20	0.85	13.65	1.68	3.51	4.89	0.23	0.89	0.70	0.10	0.38
MC09	0.06	0.02	0.04	0.06	0.05	0.05	4.39	1.05	3.04	1.00	0.29	0.62	2.71	2.00	2.18	0.43	0.24	0.36	0.30	0.10	0.15
MC10	0.05	0.02	0.03	0.06	0.04	0.05	7.06	1.84	3.93	2.11	0.41	0.99	18.75	1.94	3.99	6.63	0.28	1.04	0.70	0.10	0.28
All	0.07	0.01	0.04	0.08	0.04	0.06	8.18	0.96	3.41	2.78	0.20	0.87	18.75	1.55	3.10	6.63	0.23	0.70	0.90	0.10	0.30

Region	La (ppm)			Ce (ppm)			Pr (ppm)			Nd (ppm)			Sm (ppm)			Eu (ppm)			Gd (ppm)			Tb (ppm)		
	Max.	Min.	Ave.	Max.	Min.	Ave.	Max.	Min.	Ave.	Max.	Min.	Ave.	Max.	Min.	Ave.	Max.	Min.	Ave.	Max.	Min.	Ave.	Max.	Min.	Ave.
MC02	234	127	199	616	423	517	47.50	25.01	38.08	179	92	141	38.40	20.30	30.10	9.29	4.90	7.47	41.80	23.40	33.81	6.84	3.77	5.63
MC03	254	170	218	902	326	535	65.49	30.03	45.12	237	115	169	52.60	24.00	36.49	12.90	6.02	9.06	54.60	29.50	40.76	9.04	4.77	6.85
MC04	231	145	190	584	378	461	52.15	37.35	42.00	201	142	165	43.20	30.60	34.69	10.31	7.57	8.57	45.20	33.10	38.26	8.01	6.09	6.63
MC06	257	139	197	804	372	454	49.54	35.98	41.80	194	142	163	41.10	29.00	34.08	10.16	7.50	8.52	47.10	35.20	39.25	7.75	5.59	6.58
MC07	246	163	197	628	412	473	60.96	32.09	47.07	227	127	181	50.80	26.30	38.81	11.68	6.62	9.40	48.90	31.70	41.73	9.03	5.23	7.32
MC08	356	122	230	1260	335	592	79.22	21.28	48.70	293	73	185	58.70	13.90	38.28	13.24	3.10	8.96	64.70	18.40	39.93	9.67	2.64	6.47
MC09	312	178	246	690	392	534	68.22	32.26	51.33	266	126	209	55.00	25.90	44.35	13.24	6.54	10.01	54.70	29.90	43.58	9.03	4.47	7.28
MC10	311	174	229	1150	209	494	61.42	29.49	45.27	236	125	179	49.80	23.40	37.32	11.42	5.60	8.59	49.00	26.40	37.72	9.07	4.44	6.66
All	356	122	224	1260	209	534	79.22	21.28	46.62	293	73	180	58.70	13.90	37.91	13.24	3.10	8.94	64.70	18.40	39.70	9.67	2.64	6.67

Region	Dy (ppm)			Ho (ppm)			Er (ppm)			Tm (ppm)			Yb (ppm)			Lu (ppm)		
	Max.	Min.	Ave.	Max.	Min.	Ave.	Max.	Min.	Ave.	Max.	Min.	Ave.	Max.	Min.	Ave.	Max.	Min.	Ave.
MC02	39.80	21.80	33.19	8.48	4.75	7.12	26.20	13.80	21.46	3.87	2.06	3.15	25.20	13.90	20.79	4.01	2.19	3.37
MC03	51.50	29.80	40.26	10.30	6.87	8.63	29.80	20.60	25.76	4.33	3.05	3.79	28.70	20.00	24.99	4.45	3.27	3.93
MC04	46.10	35.80	39.16	9.27	7.28	8.18	27.50	22.90	25.06	4.11	3.46	3.77	26.00	22.10	24.00	4.11	3.64	3.87
MC06	46.40	31.90	38.96	9.96	6.73	8.22	30.10	19.40	24.80	4.55	2.84	3.72	29.50	18.40	24.10	4.73	2.99	3.86
MC07	48.80	32.10	42.87	9.62	7.03	8.83	29.20	21.10	26.84	4.31	3.33	3.96	28.40	21.20	25.60	4.40	3.29	4.02
MC08	63.30	14.10	39.19	14.40	3.02	8.03	39.60	9.57	23.42	6.32	1.46	3.54	35.00	9.77	21.53	5.93	1.67	3.50
MC09	55.30	32.30	45.12	10.50	6.98	9.23	33.10	19.40	27.29	4.71	3.35	4.14	28.50	18.40	24.63	4.65	3.13	4.03
MC10	49.40	28.50	38.33	9.95	5.93	7.90	32.40	17.10	24.41	4.43	2.57	3.53	28.30	16.60	22.36	4.47	2.56	3.64
All	63.30	14.10	39.77	14.40	3.02	8.24	39.60	9.57	24.62	6.32	1.46	3.67	35.00	9.77	22.91	5.93	1.67	3.70

The content of the major five elements show the following tendency by the type of the crusts.

- Co content is high in crusts.
- Mn/Fe is low in cobble crusts.
- Ni and Cu content is high in nodules.

The content of the five major elements show the following tendency by the position within the crust.

- The average Co, Ni, Mn, content decreases from the outer layer inward, to the inner and innermost layers. Namely the average content decreases from the surface to the deeper (substrate) parts.
- The average Cu content, on the contrary, increases from the outer layer inward, to the inner and innermost layer.
- There is no such regularity regarding the Fe content, and it is the highest in the inner layer. And the average Mn/Fe value on the contrary, is the lowest in the inner layer.

The average content of the five major elements shows the following tendency with regard to the water depth.

- Average Co, Mn content is the lowest at 2,000～3,000 m water depth, and increases with both the increase and decrease of depth.
- Average Cu content increases with the water depth.
- Average Fe content is low in both shallower than 1,500 m and deeper than 3,500 m of water.

The above tendencies regarding the chemical characteristics of the manganese crust are the result of analysis of all data, and there are naturally different tendencies in individual areas.

4) Correlation coefficients

Correlation coefficients were calculated for 31 components, namely the results of the analysis of 29 elements, Mn/Fe values, and the water depth of the sampling points. The values are shown in Table 5-4-2. The significance level value is 0.153 at 5 %.

The characteristic correlation is as follows.

- Co, Ni, Mn, Mo, Mn/Fe show mutually high positive correlation.
- Si and Al show very high positive correlation. These elements have positive correlation with Ti, Fe and negative correlation with Co, Mn, Pb, Mo, Mn/Fe.

Table 5-4-2 Correlation coefficients

	Co	Ni	Cu	Mn	Fe	Pb	Zn	Ti	Mo	V	Si	Al	Ca	P	Pt	La	Ce	Pr	Nd	Sm	Eu	Gd	Tb	Dy	Ho	Er	Tm	Yb	Lu	WD	M/F
Co	1																														
Ni	.63	1																													
Cu	-.42	.05	1																												
Mn	.73	.50	-.42	1																											
Fe	-.12	-.07	.24	-.34	1																										
Pb	.28	.05	-.17	.38	-.27	1																									
Zn	-.04	.27	.48	-.17	.37	-.17	1																								
Ti	-.04	-.12	.29	-.30	.55	-.28	.32	1																							
Mo	.45	.51	-.10	.58	-.27	.56	.07	-.41	1																						
V	.10	.27	-.08	.35	.04	-.06	.26	-.19	.37	1																					
Si	-.35	-.20	.30	-.59	.56	-.44	.12	.50	-.60	-.28	1																				
Al	-.37	-.09	.39	-.61	.44	-.55	.27	.48	-.59	-.20	.92	1																			
Ca	-.52	-.31	.19	-.52	-.45	.01	-.04	-.29	-.07	-.17	-.27	-.13	1																		
P	-.54	-.32	.21	-.54	-.41	.01	-.02	-.26	-.07	-.16	-.23	-.11	.99	1																	
Pt	-.14	.13	.39	-.26	-.06	-.31	.29	.21	-.20	.03	.01	.26	.33	.33	1																
La	-.07	-.13	.00	-.05	.02	.25	-.13	-.07	.11	-.03	-.24	-.34	.20	.22	-.19	1															
Ce	.08	-.07	.22	.04	-.17	.13	-.01	.18	.10	-.02	-.23	-.23	.18	.21	.28	.26	1														
Pr	-.02	-.21	-.04	.09	.07	.15	-.19	.03	.06	-.12	-.24	-.42	.01	.01	-.31	.61	.25	1													
Nd	.00	-.24	-.10	.09	.04	.26	-.27	-.04	.09	-.18	-.25	-.45	.02	.02	-.40	.67	.21	.97	1												
Sm	.07	-.19	-.13	.14	.08	.23	-.26	-.01	.08	-.17	-.20	-.42	-.10	-.10	-.44	.62	.17	.97	.98	1											
Eu	.09	-.14	-.20	.18	.07	.13	-.24	-.02	.06	-.11	-.22	-.42	-.11	-.11	-.43	.56	.08	.96	.95	.97	1										
Gd	.07	-.13	-.21	.17	.03	.12	-.25	-.07	.06	-.09	-.26	-.45	-.05	-.05	-.40	.56	.12	.95	.93	.93	.98	1									
Tb	.10	-.12	-.24	.18	.07	.19	-.26	-.06	.04	-.14	-.19	-.39	-.13	-.13	-.44	.49	.01	.90	.90	.92	.95	.95	1								
Dy	.12	-.14	-.30	.20	.05	.18	-.26	-.07	.08	-.11	-.26	-.45	-.10	-.10	-.48	.58	-.01	.91	.92	.93	.97	.96	.94	1							
Ho	.15	-.09	-.36	.21	.02	.17	-.27	-.12	.09	-.09	-.29	-.47	-.06	-.06	-.46	.59	-.04	.84	.87	.87	.92	.93	.91	.98	1						
Er	.14	-.11	-.39	.17	-.02	.27	-.30	-.19	.11	-.11	-.29	-.47	.00	.00	-.43	.64	-.01	.78	.84	.84	.85	.87	.90	.93	.96	1					
Tm	.18	-.09	-.41	.23	-.04	.24	-.30	-.17	.14	-.09	-.34	-.51	-.02	-.02	-.45	.61	-.04	.77	.82	.81	.85	.87	.84	.94	.98	.97	1				
Yb	.20	-.02	-.43	.23	-.02	.19	-.27	-.17	.08	-.06	-.27	-.43	-.07	-.07	-.41	.52	-.09	.70	.74	.75	.80	.83	.88	.89	.95	.97	.95	1			
Lu	.18	-.05	-.43	.18	-.04	.24	-.29	-.21	.12	-.08	-.31	-.46	.02	.02	-.38	.60	-.04	.67	.74	.73	.76	.79	.81	.87	.93	.97	.97	.97	1		
WD	-.29	-.27	.36	-.13	.06	.07	-.17	.08	-.16	-.32	.18	.02	.00	.01	-.36	.23	.22	.49	.49	.48	.42	.41	.38	.35	.24	.20	.18	.12	.09	1	
M/F	.59	.38	-.45	.88	-.72	.36	-.28	-.42	.51	.22	-.68	-.62	-.17	-.21	-.13	-.07	.09	-.02	-.01	.02	.04	.05	.05	.07	.09	.09	.14	.13	.11	-.15	1

Note WD: water depth, M/F: Mn/Fe

- Ca and P show very high positive correlation. These elements show negative correlation with Co Ni, Mn, Fe.

- Mo and Pb show high positive correlation.

- Fe and Ti show high positive correlation.

- Pt show positive correlation with Cu Ca, P, and negative correlation with Mn.

- REE, with the exception of Ce, mutually show high positive correlation. REE show negative correlation with Zn, Si, Al, Pt. Also REE show negative correlation with Cu.

- Water depth show positive correlation with Cu, REE, and negative correlation with Co, Ni, V, Pt.

5) Correlation diagram

Representative correlation diagrams of the major components which show high positive correlation are shown in Figures 5−4−2 (1), (2). In this figure, bulk samples are plotted on the left side and those of each layer of the crusts on the right side.

Co−Mn, as is seen from the bulk diagram, has high coefficient of 0.73. Regarding correlation within crust layers, it is high in all layers, but the regression coefficient (inclination of the regression line) is different for each layer, it increases from the innermost through inner to the outer layer.

Cu−Mn has negative correlation coefficient of −0.42, and show somewhat scattered dispersion. With regard to the crust layers, the outer layer has negative correlation, but the inner and innermost layers have largely scattered dispersion and correlation cannot be observed. Both bulk and crust layer data, however, appear to have two population with different regression coefficients.

Si−Mn/Fe has high negative correlation coefficient of −0.68. With regard to crust layers, the regression coefficient is almost the same for all layers and the line shifts rightward from the innermost through inner to the outer layer.

Water depth−Cu has positive correlation coefficient of 0.36, and the dispersion is somewhat scattered. With regard to the crust layers, the regression coefficient is almost the same for all layers, and the correlation is stronger in individual layers with smaller scattering than the bulk data.

6) Factor analysis

Factor analysis was carried out for 31 components of 163 samples. For estimation of communality, factor loading and factor score were calculated after normal varimax rotation. The eigen values and

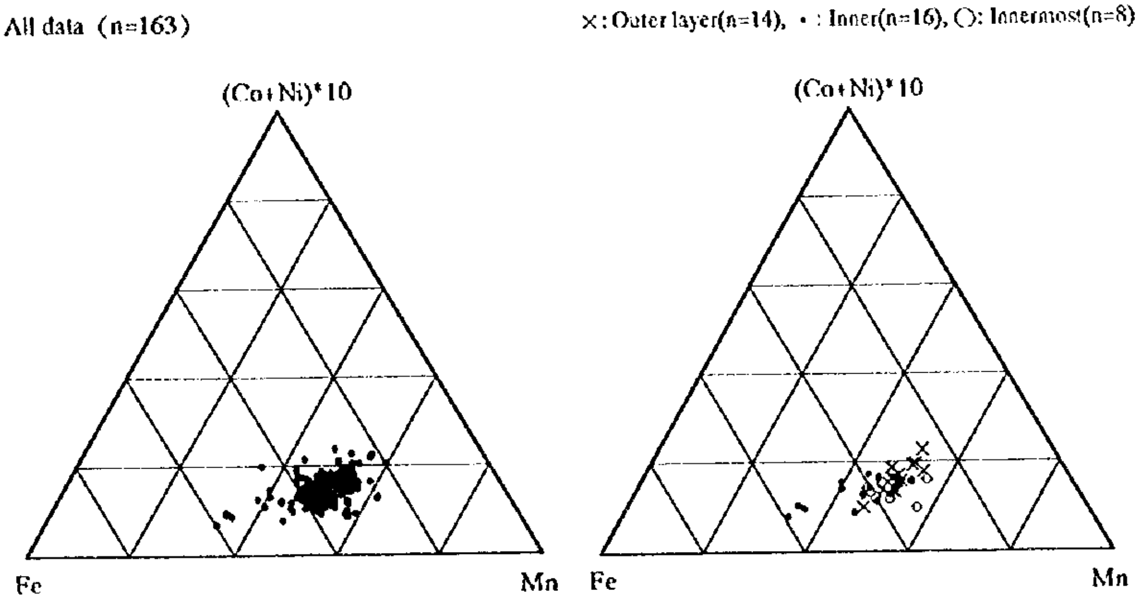

Fig. 5-4-1 (Co+Ni)*10-Mn-Fe; three components diagram

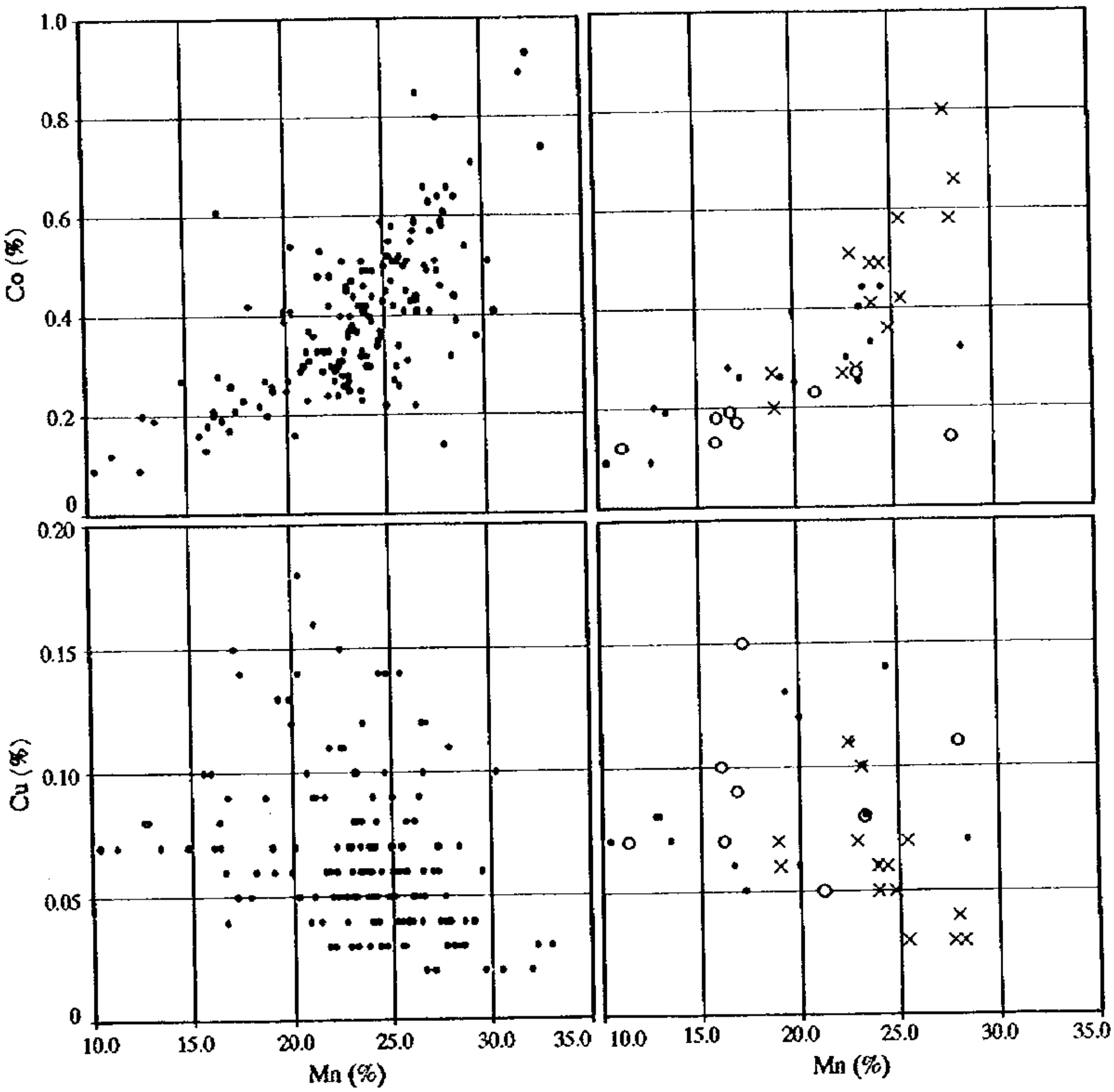

Fig. 5-4-2 (1) Correlation diagram

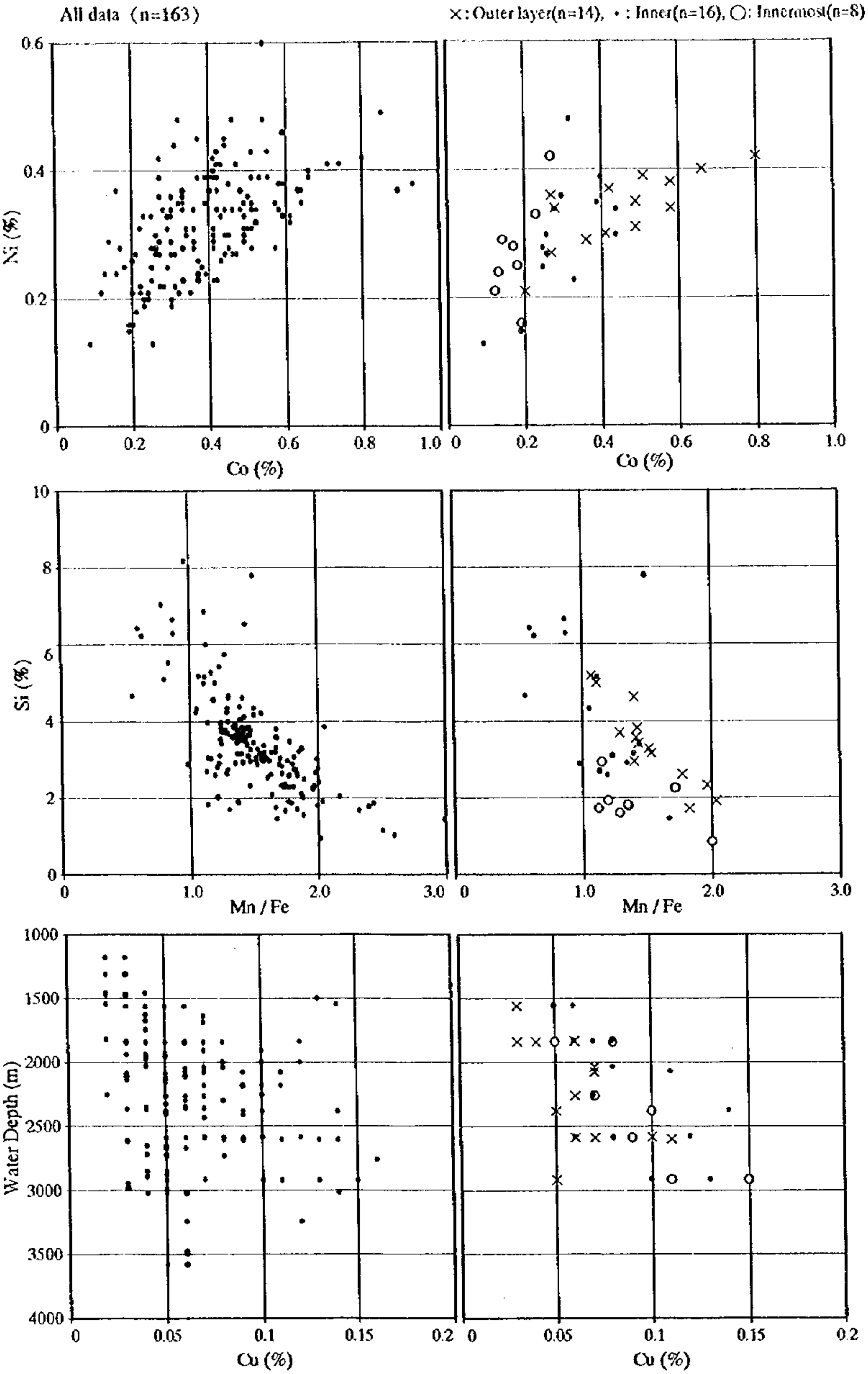

Fig. 5-4-2 (2) Correlation diagram

cumulative contribution showed the number of factors at 6. The factor loading values are shown in Table 5-4-3.

The characteristics of the five factors are as follows.

① First factor

The 13 REE components, excluding Ce, have factor loading exceeding 0.62, and these components contribute most strongly to the first factor. Pt and Al both have high factor loading of -0.49 and -0.58 respectively, and Pt contribute very most strongly to the first factor. Thus, the first factor represents the enrichment of REE and the behavior of REE has negative correlation with Pt and Al, but they are not concerned with the major components of manganese crusts. The reason for the high contribution of only REE to the first factor is that REE occupies 14 of the 31 components and also that they have a very high positive correlation mutually.

Those samples with factor scores higher than " mean value (M)+standard deviation (σ) " tend to be REE rich and Pt poor, and appear to be dominant in MC09 area. On the other hand, those samples with factor scores lower than " M- σ " tend to be REE poor and appear to be dominant in MC02, MC03, MC08, and MC10 areas.

② Second factor

Co, Ni, Mn, Pb, Mo, V have factor loading higher than 0.37, and Si, Al, Ti have loading values less than -0.47, and these components contribute most strongly to the second factor. Cu, Fe, and water depth have high factor loading of -0.54 ~ -0.41, but other factors contribute more strongly. The positive loading of the second factor indicate the enrichment of heavy metals, while the negative loading shows the enrichment of aluminosilicate minerals. Also the second factor represents the behavior of Co, Ni, Mn, Cu, Fe, the major constituents of the manganese crusts. But since the former three components and the latter two components have negative correlation, it is inferred that the concentration of Co, Ni, Mn and that of Cu, Fe occur by different cause.

Those samples with factor score exceeding " M+ σ " tend to be dominant in MC03, MC04, MC06, and MC07 areas, while those with less than " M- σ " in MC02 and MC10 areas.

③ Third factor

The factor score of Ca, P is less than -0.93, and of Fe is 0.61. These are high values and these components contribute most strongly to the third factor. Co, Si, Ti have factor score of 0.40 ~ 0.45, but these components contribute more strongly to other factors. The third factor represents the amount of carbonate and phosphate minerals contained in manganese crusts. The voids in the manganese crusts are filled with calcareous microfossil ooze and the inner layer has abundant voids and in the innermost layer veinlets of these ooze are often observed.

Table 5-4-3 Factor loadings

1st factor	Dy	Ho	Er	Tm	Gd	Eu	Tb	Sm	Nd	Yb	Lu	Pr	La	WD	Pb	Mn	Mn/Fe	Mo	Co	Ce			
	0.97	0.97	0.95	0.95	0.94	0.94	0.93	0.93	0.93	0.91	0.89	0.89	0.62	0.32	0.31	0.30	0.20	0.19	0.19	0.08			
													Ca	P	Fe	V	Ni	Ti	Zn	Cu	Si	Pt	Al
													-0.06	-0.06	-0.07	-0.08	-0.10	-0.19	-0.33	-0.35	-0.39	-0.49	-0.59
2nd factor	Mn/Fe	Mn	Mo	Co	Ni	Pb	V	Ce															
	0.88	0.85	0.68	0.68	0.55	0.42	0.38	0.00															
	Lu	Yb	Tm	Er	Pt	Ho	Zn	Dy	Tb	La	Gd	Eu	Ca	Sm	P	Nd	Pr	WD	Cu	Ti	Fe	Al	Si
	-0.01	-0.01	-0.02	-0.07	-0.08	-0.09	-0.11	-0.14	-0.17	-0.17	-0.18	-0.19	-0.20	-0.22	-0.23	-0.24	-0.27	-0.41	-0.44	-0.48	-0.54	-0.61	-0.69
3rd factor	Fe	Si	Co	Ti	Al	Ni	Mn	Zn	Tb	V	Eu	Dy	Yb	Ho	Sm	Gd	Tm						
	0.62	0.45	0.43	0.41	0.33	0.31	0.30	0.16	0.12	0.11	0.10	0.09	0.08	0.06	0.06	0.04	0.00						
										Er	Lu	WD	Pr	Mn/Fe	Nd	Mo	Cu	Pb	La	Pt	Ce	P	Ca
										-0.01	-0.02	-0.03	-0.04	-0.06	-0.06	-0.08	-0.12	-0.18	-0.24	-0.28	-0.31	-0.93	-0.94
4th factor	Ce	Cu	Zn	Mo	Ti	Pr	Ni	WD	Pt	Nd	La	Sm	Fe	V	Pb	Mn	Co	Eu	Gd	Tb			
	0.62	0.62	0.43	0.32	0.29	0.29	0.28	0.28	0.26	0.21	0.20	0.19	0.16	0.15	0.14	0.12	0.12	0.12	0.10	0.01			
													Mn/Fe	Dy	P	Ca	Ho	Al	Er	Tm	Si	Yb	Lu
													-0.01	-0.02	-0.05	-0.07	-0.10	-0.14	-0.15	-0.16	-0.17	-0.22	-0.23
5th factor	Zn	V	Pt	Ni	Fe	Lu	Yb	P	Tm	Ca	Er	La	Ho	Mo	Co	Dy	Al	Cu	Ti	Gd			
	0.47	0.35	0.34	0.34	0.27	0.27	0.24	0.18	0.18	0.17	0.17	0.15	0.15	0.12	0.05	0.04	0.02	0.02	0.02	0.00			
													Tb	Eu	Pr	Nd	Si	Sm	Mn	Ce	Pb	Mn/Fe	WD
													-0.02	-0.04	-0.07	-0.11	-0.13	-0.13	-0.15	-0.19	-0.21	-0.24	-0.57
6th factor	Mo	Pb	Fe	V	WD	Cu	Zn	La	Nd	Si	P	Sm	Ca										
	0.37	0.32	0.21	0.20	0.19	0.18	0.17	0.07	0.02	0.02	0.01	0.01	0.00										
						Dy	Er	Ni	Tb	Tm	Ho	Eu	Pr	Lu	Gd	Mn	Al	Yb	Mn/Fe	Co	Ti	Ce	Pt
						-0.01	-0.01	-0.01	-0.02	-0.03	-0.03	-0.03	-0.05	-0.05	-0.06	-0.07	-0.08	-0.08	-0.21	-0.26	-0.33	-0.40	-0.46

	Co	Ni	Cu	Mn	Fe	Pb	Zn	Ti	Mo	V	Si	Al	Ca	P	Pt
1st factor	0.19	-0.10	-0.35	0.30	-0.07	0.31	-0.33	-0.19	0.19	-0.08	-0.39	-0.59	-0.06	-0.06	-0.49
2nd factor	0.68	0.55	-0.44	0.85	-0.54	0.42	-0.11	-0.48	0.68	0.38	-0.69	-0.61	-0.20	-0.23	-0.08
3rd factor	0.43	0.31	-0.12	0.30	0.62	-0.18	0.16	0.41	-0.08	0.11	0.45	0.33	-0.94	-0.93	-0.28
4th factor	0.12	0.28	0.62	0.12	0.16	0.14	0.43	0.29	0.32	0.15	-0.17	-0.14	-0.07	-0.05	0.26
5th factor	0.05	0.34	0.02	-0.15	0.27	-0.21	0.47	0.02	0.12	0.35	-0.13	0.02	0.17	0.18	0.34
6th factor	-0.26	-0.01	0.18	-0.07	0.21	0.32	0.17	-0.33	0.37	0.20	0.02	-0.08	0.00	0.01	-0.46

	La	Ce	Pr	Nd	Sm	Eu	Gd	Tb	Dy	Ho	Er	Tm	Yb	Lu	Mn/Fe	WD
1st factor	0.62	0.08	0.89	0.93	0.93	0.94	0.94	0.93	0.97	0.97	0.95	0.95	0.91	0.89	0.20	0.32
2nd factor	-0.17	0.00	-0.27	-0.24	-0.22	-0.19	-0.18	-0.17	-0.14	-0.09	-0.07	-0.02	-0.01	-0.01	0.88	-0.41
3rd factor	-0.24	-0.31	-0.04	-0.06	0.06	0.10	0.04	0.12	0.09	0.06	-0.01	0.00	0.08	-0.02	-0.06	-0.03
4th factor	0.20	0.62	0.29	0.21	0.19	0.12	0.10	0.01	-0.02	-0.10	-0.15	-0.16	-0.22	-0.23	-0.01	0.28
5th factor	0.15	-0.19	-0.07	-0.11	-0.13	-0.04	0.00	-0.02	0.04	0.15	0.17	0.18	0.24	0.27	-0.24	-0.57
6th factor	0.07	-0.40	-0.05	0.02	0.01	-0.03	-0.06	-0.02	-0.01	-0.03	-0.01	-0.03	-0.08	-0.05	-0.21	0.19

Note WD: water depth

Those samples with factor score less than "M− σ" are restricted to MC08 and MC10 areas, and almost all of them are in the innermost layer. Those samples with factor score higher than "M+ σ" are dominant in MC02 and are rich in Si, Ti, Fe.

④ Fourth factor

Cu and Ce have high factor score of 0.61 and contribute most strongly to the fourth factor. Zn has factor score of 0.42 which is high, but its contribution to other factors are stronger. There are no component with high negative score. The fourth factor indicate the enrichment of Cu and Ce, but their correlation coefficient is 0.22 and not high.

Those samples with factor score higher than "M+ σ" are enriched in Cu and Ce, and these samples are almost all from MC08 area. The reason for high content of Cu in MC08 area, but it is inferred that the different geloogic structure of the area and the older age of the seamount are significant factors.

⑤ Fifth factor

Zn has a factor score of 0.47 and the water depth 0.56 and these components contribute most strongly to the fifth factor. Ni, Pt, and V have factor score of 0.33 ~ 0.35, but they contribute more strongly to other factors. The positive loading of the fifth factor indicate the enrichment of Zn and the negative loading the increase of water depth of the sampling point.

Those samples with factor loading higher than "M+ σ" indicate the enrichment of Zn and Pt and are dominantly in MC02, MC03, MC08. On the other hand, those samples with factor loading less than "M− σ" occur dominantly in MC08, MC09, MC10. The water depth of MC08 ~ MC10 is deeper than in MC02 ~ MC04.

⑥ Sixth factor

There are no component which contribute most strongly to the sixth factor. Components which contribute secondly to this factor are Pt with −0.45 loading, Ce with −0.40, Mo with 0.37 and Pb with 0.32. The negative loading of the sixth factor indicate the enrichment of Pt, but other factors probably also ply some role.

Those samples with factor score less than "M− σ" occur dominantly in MC02, MC03, MC04, MC07 and tend to be rich in Pt.

5-5 Mineral Composition

Polished sections were prepared for dredged samples with appropriate thickness and with notable layered structure. These were studied by reflection microscopy. The number of samples studied is two nodules and one cobble crust. The result of the study is laid out in Table 5-5-1 and representative photographs are shown in Figures 5-5-1 (1), (2).

The main constituents of manganese crusts are manganese and iron oxides. The kinds of manganese oxides which occur on the seafloor differs by the shape (crusts, nodules, chimneys, etc.,) and their genetic environment (seamounts, deep seafloor, volcanoes, etc.). The manganese minerals which comprise manganese crusts are; todorokite, buserite (10 Å manganite), birnessite (7 Å manganite), vernadite (δ $-MnO_2$).

The identified manganese minerals are vernadite and todorokite. The mode of occurrence differs by individual samples and the position within the crust. Banded and kidney textures are developed in the black compact parts, while it tends to have prismatic, granular, and colloform texture in parts associated with many brown oxides. The following is the description of the samples. Sketch of the observed surface are shown in Figures 5-5-2 ~ 5-5-4, the figures on the left show the detailed layer division (I ~ X), and those on the right show the location of the photomicrographs and the numbers (1 ~ 25).

1) 97SMC08CB04-P1 (Fig. 5-5-1, Photos A ~ D)

The sample is a nodule with 4 cm diameter, it has a 2 cm core of hyaloclastite in the center. The nodule was cut perpendicular to the long axis and the cut surface was observed. The manganese crust has a total of about 1 cm thickness around the core.

The nodule is divided into I ~ IV zones from the center outward. Zone I is the hyaloclastite core, and the voids are filled by colloform todorokite (Photo D). Zone II is banded and colloform todorokite show prismatic occurrence (Photo C). Zone III is similar to Zone II, but is wider (Photo B). Zone IV consists of colloform todorokite forming compact banded texture (Photo A).

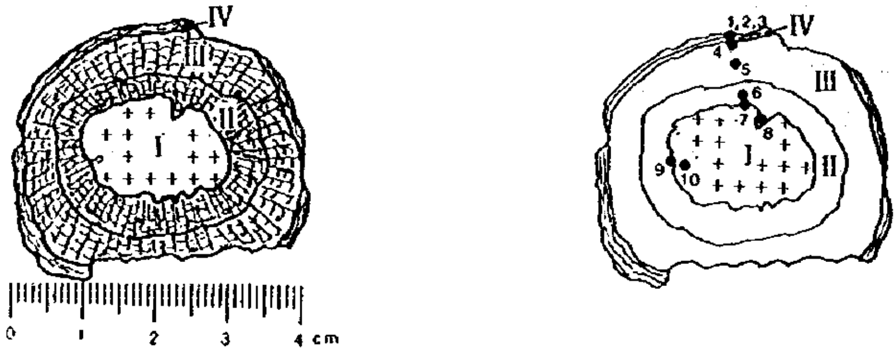

Fig. 5-5-2 Sectional illustrations of polished sample

Table 5-5-1 Results of microscopic observation for manganese crusts polishes

Sampling site No.		97SMC08CB04	97SMC08CB04	97SMC08CB08
Sample code No.		P1	P2	P1
Crust type		Nodule	Nodule	Cobble crust (Only the thickest part observed)
Thickness (mm)		9 ~ 11	14 ~ 22	65
Substrate rock		Hyaloclastite (rounded pebble)	not exist Two center cores exist.	not exist Small grain of phosphorite is included in the center.
Zonage		four zones (Ⅰ to Ⅳ) Ⅰ zone is the rock core.	five zones (Ⅰ to Ⅴ)	ten zones (Ⅰ to Ⅹ)
Discontinuous plane		existing in the boundary of each zones	existing in the boundary of each zones	existing in the boundary of each zones
Minerals occurred		Todorokite >> Vernadite Hydroxide, Collophane	Vernadite > Todorokite Hydroxide, Collophane	Vernadite >> Todorokite Hydroxide, Collophane
Todorokite	Occurrence	main in the every zones	only in the outermost zone	very rare
	Amount	abundant	a little	little
	Crystal grain	very fine	very fine	very fine
	Crystallinity	microcrystalline to cryptocrystalline	microcrystalline to cryptocrystalline	microcrystalline to cryptocrystalline
	Texture	colloform, banded, reniform, columnar	colloform, banded	colloform
Vernadite	Occurrence	very rare	main in the every zones	main in the every zones
	Amount	little	abundant	abundant
	Crystal grain	very fine	very fine	very fine
	Texture	colloform, banded, dendritic, granular, filling cracks	colloform, banded, granular, dendritic, reniform, columnar, irregular massive, irregular network	colloform, banded, granular, dendritic, reniform, columnar, irregular massive, irregular network
Remarks				Ⅱ and Ⅲ zones are amorphous ?

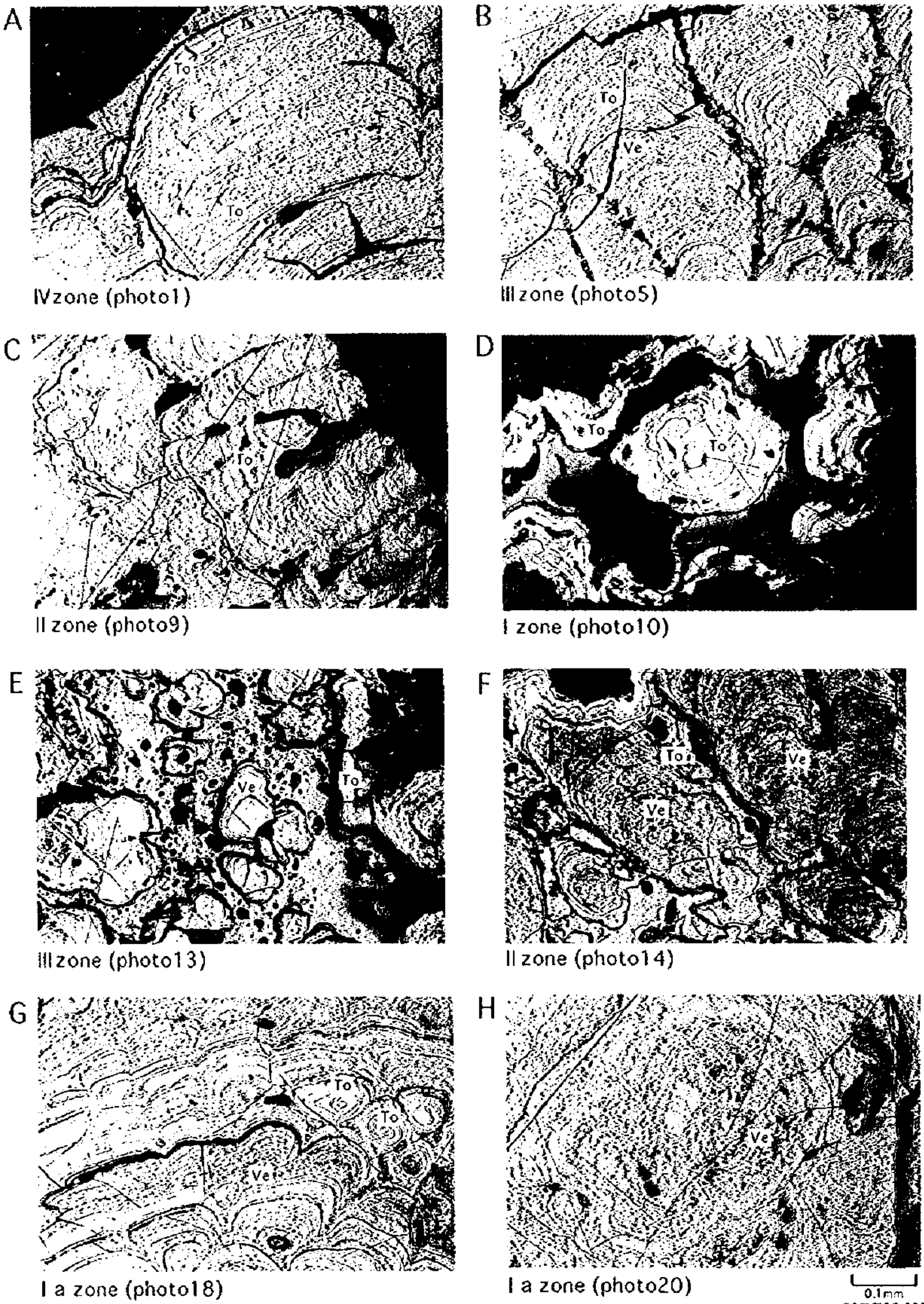

A: IVzone (photo1)
B: III zone (photo5)
C: II zone (photo9)
D: I zone (photo10)
E: III zone (photo13)
F: II zone (photo14)
G: I a zone (photo18)
H: I a zone (photo20)

Note: A~D are from 97SMC08CB04-P1, E~H are from 97SMC08CB04-P2.

Legend To:Todorokite, Ve:Vernadite

Fig. 5-5-1(1) Photographs of microscopic observation of manganese crusts polishes

J

IXzone (photo4)

K

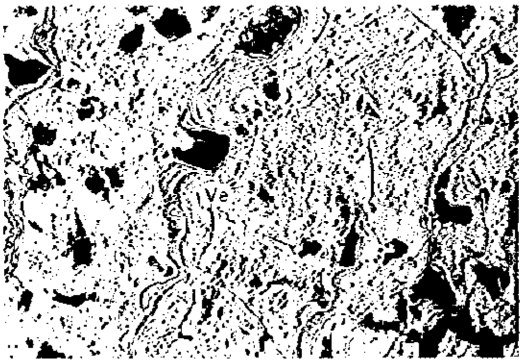

VIIIzone (photo7)

L

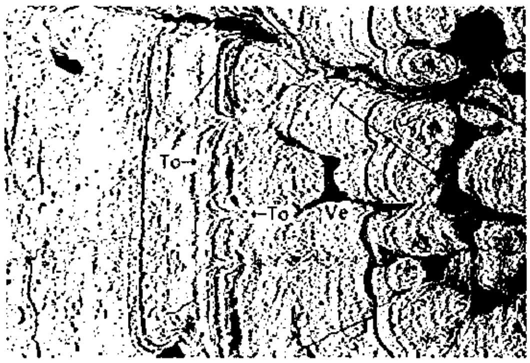

VIzone (photo10)

M

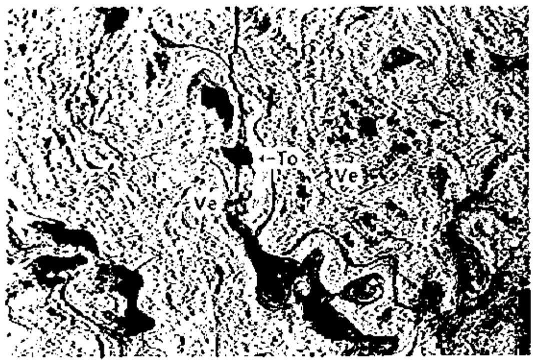

IVzone (photo14)

N

II zone (photo17)

P

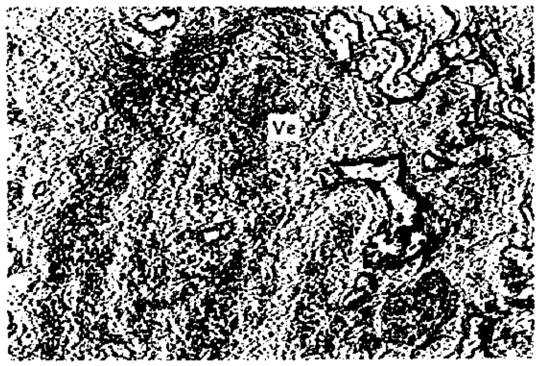

II zone (photo18)

Q

II zone (photo20)

R

I zone (photo22)

0.1mm
common scale

Note: J~R all are from 97SMC08CB08-P1.

Legend To:Todorokite, Ve:Vernadite

Fig. 5-5-1(2) Photographs of microscopic observation of manganese crusts polishes

Whole Zone II to IV consists of todorokite and vernadite is almost non-existent. Todorokite consists of two types with different reflectivity and color tone. Both have high reflectivity and is not anisotropic and thus is inferred to be microcrystalline to cryptocrystalline todorokite. Clastic and authigenic minerals occur in Zones II and III, they are more abundant in II.

2) 97SMC08CB04-P2 (Fig. 5-5-1 (1), Photos E ~ H)

The sample is a nodule with 4.5 cm diameter and it does not have a core of rock fragments. The nodule was cut perpendicular to the long axis and the cut surface was observed. The manganese crust has a thickness of 1.4 ~ 2.2 cm.

The nodule is divided into I ~ IV zones from the center outward. Zone I is subdivided into Ia and Ib. It is noted with unaided eyes that Zone I is compact with layered texture, Zones II and III consists of brown oxide minerals in radial form, and Zone IV is compact and layered. These three correspond to innermost, inner, and outer layers.

Zone I consists mainly of vernadite with banded, spherical, dendritic, and kidney texture, and minor amount of thin layers of colloform todorokite is intercalated (Photo G). In Zone I there are two cores (Photo H). The minerals composition and the texture is the same for Ia and Ib, but there is a thin (about 0.1 mm) layer of most probably phosphate mineral intercalated between the two subzones. Zone II consists mainly of prismatic and spherical vernadite and fills the interstices of colloform prisms of todorokite and vernadite (Photo F). Zone III contains minor amount of colloform todorokite with scattered banded and spherical vernadite (Photo E). Zone IV contains compact bands of colloform of minute todorokite.

The major constituent of Zones I ~ II is vernadite and that of Zone IV todorokite. Layered texture is prevalent in Zones I and IV, and prismatic texture in Zones II and III. Zone III is porous, while in Zones II and III clastic material and authigenic minerals are abundant. The width of the growth bands is 5 ~ 50 μ m.

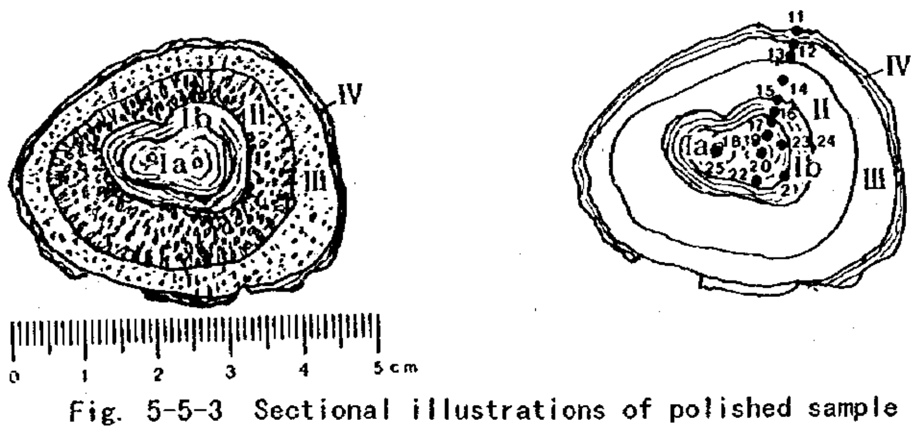

Fig. 5-5-3 Sectional illustrations of polished sample

3) 97SMC08CB08-P1 (Fig. 5-5-1 (2), Photo J ~ R)

The sample is cobble crust with 13 cm long axis without rock fragment core. The sample was cut parallel to the long axis, and the upper part with the thickest crust was observed. The manganese crust is 6.5 cm thick.

The crust is divided into zones I ~ X from the center outward. It is seen with the unaided eyes that; Zones I to IV are compact with layered texture, V to VII and IX contains network of brown oxides, and VIII and X are compact and layered. Zones I to IV correspond to the innermost layer, V to VIII the inner layer, and IX and X the outer layer.

Zone I has spherical shape with 1 cm diameter consisting mostly of banded colloform vernadite with intercalation of minute mount of thin colloform todorokite (Photo R). There are two minute irregular clusters which are inferred to be phosphate minerals. In Zone II, colloform vernadite forms spheres and bands, and network of hydroxides or phosphate minerals are developed (Photo N ~ Q). Zone III consists mainly of bands and spheres of vernadite.

Zones IV to X consists of alternation of layers of compact thin layered texture (Zones IV, VI, VIII, X) and layers rich in brown network veins (Zones V, VII, IX). The latter layers contain many clastics and authigenic minerals, and Zones VII and IX are porous.

Zone IV consists of irregular colloform vernadite with small amount of colloform todorokite. In Zone VI, colloform vernadite occur in banded and kidney texture accompanied by minute amount of todorokite. Zones VIII and X consist of colloform vernadite.

Zone V consists of irregular network and irregular massive colloform vernadite. In Zones VII and IX, banded colloform vernadite occur sporadically with partly irregular network and irregular massive colloform vernadite.

Zones I to X consists mainly of vernadite and todorokite is very rare. However, the minerals identified as vernadite in Zones II and III have low reflectivity and the possibility of amorphous impure ferromanganese hydroxides cannot be denied.

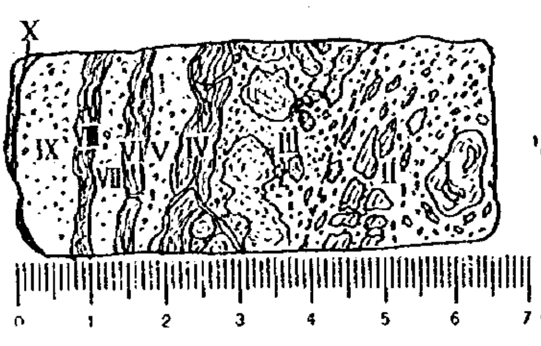

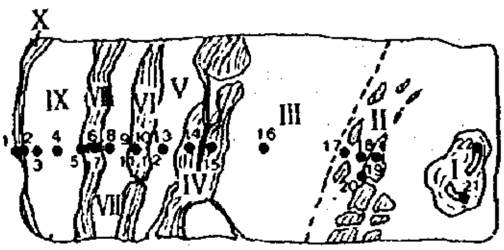

Fig. 5-5-4 Sectional illustrations of polished sample

5-6 Growth Rate of Manganese Crusts

Concentration of ^{10}Be was measured in order to determine the growth rate of manganese crusts. Three samples were studied and nine to twelve points of different depth were measured for each sample. The measurement was carried out for 30 points. The results are shown in Table 5-6-1.

The samples were, after grinding, kept at 120°C for 12 hours for drying and constant weight was confirmed. One mg of ^{9}Be was added as carrier to 1 g of sample. Tandem accelerator and accelerator mass spectrometer were used for the measurement of ^{10}Be.

The rate of the growth of the crust is obtained under the assumption that the ^{10}Be concentration in sea water is constant and that its behavior does not change during the formation of the manganese crust. Since the ^{10}Be concentration increases from the deeper part of the crust outward, the rate of growth is calculated from the depth of the measuring point and the ^{10}Be concentration curve.

Outer layers have enough high contents of ^{10}Be but inner and innermost layers have very low contents in every three samples, so that the growth rate of whole layers were not calculated. In 97SMC08 CB02, outside six points data show that the growth rate is 2.2 mm/Ma and that the sixth point age is 12 million years. In 97SMC10CB06, outside three points data show that the growth rate is 7.1 mm/Ma and the third point age is 7.5 million years. In 97SMC10CB07, outside two points data show that the growth rate is 1.4 mm/Ma and the second point age is 9 million years. In result, the outer layer parts with the thickness of 22 to 40 mm have been created from 7 to 9 million years ago.

Though the growth rate of inner and innermost layers were not calculated, that of inner layer is estimated to be almost same as outer layer's as the inside two of outside six points belong to the inner layer in 97SMC08CB02. Supposing the growth rate of whole layers is 2.2 mm/Ma, a crust 10 cm thick has been created for 45 million years.

In the areas of MC03, MC04, MC06, MC07, and MC09 where manganese crusts are thin and have only outer layer, the thickest crusts are 14 to 47 mm thick and the basalt age are 5 to 14 Ma. In the areas of MC08 and MC10 where manganese crusts are thick and composed of some layers, the thickest crusts are 90 to 155 mm thick and the basalt age are 24 to 70 Ma. Therefore the age of manganese crusts calculated from the growth rate is harmonized with the age of substrate basalt.

Still, Sharma and Somauajulu (1982) reported that the growth rate of manganese crusts in the Pacific region was one to eight mm/Ma, and JICA-MMAJ (1997) 2.6 to 5.2 mm/Ma in the Marshall Islands sea area.

Table 5-6-1 Results of ^{10}Be isotopic analysis for manganese crusts

Sampling site No.	Code	Crust type	Crust layer	Depth (mm)	10Be content (10^8 at/g)	Growth rate (mm/Ma)	Age formed (Ma)	Residue (%)
97SMC08CB02	B1	Cobble crust	Outer	0 ～ 7	288.2		(0)	2.9
			Outer	7 ～ 12	100.2			1.1
			Outer	12 ～ 17	30.98	2.2		1.2
			Outer	17 ～ 22	10.85			4.2
			Inner	22 ～ 28	4.298			3.3
			Inner	28 ～ 36	0.709		12	5.5
			Inner	36 ～ 45	1.396	unknown		1.4
			Innermost	45 ～ 52	0.1634			1.4
			Innermost	52 ～ 62	0.1442			3.0
97SMC10CB06	B1	Crust	Outer	0 ～ 17	85.0		(0)	13.7
			Outer	17 ～ 30	31.27	7.1		19.9
			Outer	30 ～ 42	13.99		7.5	21.5
			Inner	42 ～ 55	9.828	unknown		20.1
			Inner	55 ～ 68	9.995	(reverse)		19.1
			Inner	68 ～ 79	16.04			9.8
			Inner	79 ～ 89	48.93			11.5
			Inner	89 ～ 100	193.6			12.4
			Inner	100 ～ 110	257.2			7.7
97SMC10CB07	B1	Cobble crust	Outer	0 ～ 10	101.0	1.4	(0)	3.6
			Outer	10 ～ 30	5.452		9	18.2
			Inner	30 ～ 50	0.6538	unknown		12.2
			Inner	50 ～ 75	0.9438			16.0
			Inner	75 ～ 95	0.02112			10.6
			Inner	95 ～ 115	0.2423			5.4
			Inner	115 ～ 135	0.3599			5.5
			Innermost	135 ～ 145	1.022			2.7
			Innermost	145 ～ 150	0.8331			3.9

5-7 Occurrence of Manganese Crusts

The occurrence of manganese crusts in the areas surveyed is summarized in Table 5-7-1. The factors regarding the occurrence of manganese crust deposits are; size of seamounts, relief and topography of seamounts, average gradient of the upper to middle slope of the seamounts, water depth of the seamount summit, exposure ratio of the manganese crusts, thickness of the crusts and average grade of the major elements, reserve of the manganese crusts. The following materials and data were used for the assessment of the above factors, namely seafloor topographic maps for the relief of the seamounts, MBES acoustic pressure images for the exposure ratio of the crusts, size of the seamounts, exposure ratio, and thickness for the reserve of the manganese crusts. For factors other than the above, actual measured values are shown.

Good exposure of manganese crusts on the seamount slopes is in MC04, MC05, MC10 areas. The thickness of the manganese crusts, however, is very thin in MC04 and MC05 areas. The crusts are thick in MC02, MC08, and MC10 areas. In these areas, however, the cobalt content is low. Also in MC02 area, the manganese crusts are exposed in a narrow and limited locality. The MC09 area where the cobalt grade is high, the summit is deep and the topographic relief is rugged. The MC06 are where the nickel grade is high, the seamounts are small and the average thickness is thin. Thus each area surveyed all have relatively favorable and unfavorable factors.

Considering all above factors, it is concluded that MC08 and MC10 areas are most promising and the difference with other areas is considerable.

Table 5-7-1 Occurrences of manganese crusts

Region	Scale of seamount	Topography of seamount			Crust exposure		No. of site	Crust thickness (mm)		Average			Amount of crust	Remarks
		Roughness	Gradient of flank	Depth of summit	Flat summit	Flank		Maximum	Average	Co (%)	Ni (%)	Pt (ppm)		
MC02	moderate	a little	7°	1,080 m	low	moderate	4	50	21	0.35	0.33	0.50	a little	
MC03	moderate	a little	15°	510 m	–	moderate	12	47	8	0.48	0.36	0.33	a little	
MC04	moderate	moderate	10°	100 m	–	high	17	20	1	0.47	0.32	0.23	little	two seamounts
MC05	moderate	moderate	16°	190 m	–	high	7	< 1	< 1	–	–	–	none	
MC06	small	moderate	17°	740 m	–	moderate	8	20	3	0.47	0.36	0.28	a little	
MC07	moderate	moderate	12°	1,420 m	low	moderate	10	14	5	0.48	0.31	0.19	a little	
MC08	big	moderate	18°	1,580 m	low	moderate	18	90	20	0.36	0.32	0.37	abundant	northern seamount
MC09	moderate	abundant	17°	2,030 m	–	moderate	13	23	7	0.49	0.30	0.14	a little	northern seamount
MC10	big	moderate	12°	1,560 m	low	high	16	155	20	0.33	0.36	0.27	abundant	southern seamount

Chapter 6 Discussions

6-1 Evolution of Seamounts and Occurrence of Manganese Crusts

It was clarified from the results of sampling in the nine areas from MC02 to MC10 that the occurrence of the manganese crusts differ greatly in each area. This is mainly caused by the difference of the geologic environment of the seamounts by areas. Each seamount was formed on different geologic structure, and the outline of their evolution is as follows.

The seamounts in the MC08 and MC10 areas were formed as oceanic islands by the alkaline basalt volcanic activities during Mesozoic to Paleogene. After the cessation of the volcanism, they became atolls by erosion and subsidence of the ocean floor, then the islands submerged below water during Neogene by continuing subsidence and they presently exist as guyots. The seamounts in the MC07 area are annular and were formed during Neogene, and the eastern, western, and northern sides of the annular body have flat summits similar to those in the MC08 area. The northern seamount in the MC09 area was formed in Neogene, but its summit was rarely above the water and the present summit consists of many peaks. The summits of the seamounts in the above four areas are deeper than 1,400 m and reef limestone was not collected.

The seamounts in MC05 and MC06 areas were formed by Neogene alkaline basalt volcanic activities as oceanic islands and are presently pointed seamounts with shallow summits. The MC03 seamounts were formed by Neogene tholeiite ~ alkaline basalt volcanism and those in MC04 area by tholeiite ~ mid-oceanic ridge basalt activities of the same period. They are presently ridge-type pointed seamounts. The seamounts in MC02 area were formed by mid-oceanic ridge basalt volcanism and are presently oceanic plateau-type table seamount. The summits of the seamounts of the above five areas are shallower than 1,100 m, and reef limestone extend widely from the summit to the upper slopes.

The relation between the topography of the seamounts and the thickness of the manganese crusts can be summarized as follows.

- The crusts of guyots older than Paleogene (MC08, MC10 areas) are thick and developed, while those of younger seamounts (MC05, MC07 and other areas) are thin.
- The thickness of crusts on seamounts younger than Paleogene depends more on the topography and geology of the seamount rather than the age.
- Reef limestone is dominant on seamount slopes shallower than 1,800 m, and crusts are thin on these seamounts (MC03 ~ MC06 areas).
- Pointed seamounts with very shallow summits (MC04, MC05 areas) have thin crusts.

The diversity of the shape of seamounts, age of seamounts, thickness of manganese crusts, water depth of the sampled crusts are also apparent in their chemical composition. Since in the statistical analysis of the chemical results processes all data together, this diversity must have greatly affected the analytical results. In some of the correlation of major elements, tendencies different from those of the Marshal Islands EEZ (JICA--MMAJ, 1997) are observed. In the present survey the basic statistical data were calculated for various divisions, but later if sufficient data becomes available, comparative study of multi--variable analysis by areas would be of significance.

Although not in detail, it was possible to acquire important data and knowledge regarding the occurrence of manganese crusts and the development of the seamounts in the FSM waters. It would be very desirable, on the basis of these newly acquired knowledge, to carry out further exploration mainly in the northern to northwestern part of the survey area where old guyots with developed manganese crusts are distributed. It is also necessary to further accumulate large amount of data in order to clarify the formation of manganese crusts in this area.

6-2 Possibility of Hydrothermal Sulfide Mineralization in the Area

A hydrothermally altered basalt sample was recovered from the lower northern slope of a seamount in the MC02 area. Greenish dark gray altered basalt has been wholly chloritized and carbonatized and, in places, weak pyrite dissemination occurs along calcite veinlets. Similar alteration and dissemination has been reported from almost the same locality by USGS-KORDI (1992). The northern slope of this seamount is steep and linear in the east-west direction, and there a graben extends in the same direction to the north. It is believed that this slope and graben were formed in association with the tectonic movement of the ocean floor, and that the hydrothermal alteration occurred simultaneously. The fact that the basalt of this locality has MORB composition, supports the possibility that the zone between the northern slope of the seamount and the graben to the north contain hydrothermal sulfide mineralization similar to those in the mid-oceanic ridges.

Similar geologic structure as well as lateral faults transecting the seamount is observed in the northern side of the seamount in MC03. Also " *Munidopsis* " sp., which is a hydrothermal creature was caught at the saddle of the central part of the seamount immediately above these faults.

As reported above, there is a large geologic structure in the MC02 and MC03 areas and hydrothermal alteration has been confirmed. Thus existence of hydrothermal sulfide deposits is anticipated.

6-3 Effectiveness and Accuracy of Seafloor Topographic Maps prepared by Satellite Altimetry

In planning the present survey, ETOP05 and 5' × 5' grid data of Terrain Base Seafloor Topographic File by NOAA were used for selecting the target seamounts. Since this data file is a compilation of all the past seafloor topographic data, it includes those from the days when NNSS was used for positioning, and thus there have been cases when reported seamounts could not be located in some areas. And it was feared that in FSM area, where past surveys have been few, the accuracy might be lower than in other areas.

SOPAC Secretariat had offered before the present survey, the use of the "French Government, Ministry of Foreign Affairs, Satellite Bathymetric Survey of Maritime Zone of the State if Yap FSM, June, 1996". Also "Smith, W.H.F., and D.T. Sandwell, Global Seafloor Topography from Satellite Altimetry and Ship Depth Soundings, submitted to Science, April 7, 1997" could be used as reference. From the above, it was confirmed that the use of inferred seafloor topographic maps from satellite altimetry is very effective method for estimating the location of seamounts.

By comparing the seafloor topographic maps prepared by the present survey and the satellite isobathymetric map, it is seen that the outline of the shape and the location of the seamounts are sufficiently accurate for use in planning surveys. The water depth figures shown need to be treated with care.

As satellite topographic data are expected to be used not only in survey planning, but in many fields of activities, it is desired that efforts be made to increase the accuracy by clarifying and incorporating the regional geoscientific characteristics.

Chapter 7 Summary

The third year of the third phase of the five-year SOPAC Program, topographic surveys sampling for manganese crust deposits were carried out in the exclusive economic zone of the Federated States of Micronesia. The duration of the survey cruise was 74 days.

There are some oceanic islands, atolls and many seamounts in the survey area. These occur along two large oceanic ridges in the western side, namely the Yap Zone ~ Truk Zone, on the eastern side these occur together with the oceanic islands which are scattered in the east-west direction.

The survey was composed mainly of topographic cruise of each seamount in order to prepare detailed topographic map by MBES, Seafloor observation by FDC, and of sampling by chain back dredge (CB), arm dredge (AD), and large corer (LC) with the objective of confirming the mode of occurrence of the crust deposits. The continuity of the deposits, the type, thickness, grade, exposure ratio, and other relevant features of the manganese crusts were clarified by seafloor observation and sampling. Important samples were studied in laboratories on land by various methods including; various analyses, X-ray diffraction, and microscopy. These together with the results of onboard analysis provided the basis for integrated analysis of the resource. nSBP survey was carried out together with MBES, and for some of the seamounts, SSS survey was conducted for understanding the micro topography of the seafloor.

(Topographic survey)

Efforts were made to select seamounts of diverse nature for the survey, therefore, water depth, size, location and various other relevant factors were considered. During Leg 1, six areas in the western to the southern part were studied. During Leg 2, four areas in the eastern to the northern part of the survey area were surveyed. Thus a total of ten areas were the target of investigation. As the seafloor topography of the survey area is complex, the type of the seamounts are diverse and they are; three guyots, one pointed seamount, two oceanic ridge types, two high relief types, and one shoal.

The areal extent of the survey differed by the size of the seamount and the results, but it was generally 20 × 30 miles for each seamount. For all seamounts, the survey provided detailed topography and formed the basis for sampling and other subsequent studies.

The water depth of the seamount summits ranges widely from (10 *1) to 2,032 m, the relative height ranges from 2,400 m to 4,000 m and the largest seamount is MS10 extending 43 km east-west and 43 km north-south.

(MBES acoustic images)

In MBES acoustic images dark colored parts corresponding to exposed rocks are observed in all seamounts on, summits, ridges on the slopes, and the valleys, in other words in areas where the slope is steep. On the slopes, the images become pale downward, indicating the tendency of gradually increasing unconsolidated sediment thickness. On the other hand, pale image color corresponding to unconsolidated sediments are observed in parts with low relief such as the flat summits.

Exposed rocks of seamounts are often covered by crusts. Therefore, the distribution of exposed rocks estimated by MBES acoustic images possibly show the distribution of manganese crusts. Seamounts with flat summit covered by unconsolidated sediments such as those often seen in the central Pacific, are four seamounts in MC02, MC-07, MC08, and MC10. For other seamounts, it was inferred that exposed rocks or pebbly materials are distributed in most of the summit to the slope.

(nSBP survey)

There were four seamounts, MC02, MC07, MC08, and MC10 where unconsolidated sediments were clearly observed by SBP survey, this agrees with the distribution of unconsolidated sediments obtained by MBES acoustic images. The latter three seamounts are guyots, and SBP records show that T-type is clearly developed. In seamount MC10, T-type is most developed and is distributed widely to the periphery. It is inferred from correlation with the results of seafloor observation by FDC that the acoustically transparent layer distribution corresponds to that of unconsolidated sediments, and their thickness ranges from 20 to 40 m.

(SSS survey)

It has been shown that SSS images can clarify the variations of micro topography and the bottom sediments in more detail than the MBES acoustic reflection intensity distribution. In the present survey, data regarding the two-dimensional conditions regarding the rock exposures on pinnacle slopes, nodule distribution at the foot of the pinnacles, rock exposures at the shoulders where the gradient somewhat increases, and the rock exposures on upper slopes.

In the SSS images, it has been clarified that the high acoustic reflection intensity is correlated to exposed rocks confirmed by FDC observation, and similar results were obtained from the present survey. And further details were clarified concerning distribution of exposed rocks and pebbles which cannot be interpreted from MBES data such as local low acoustic reflection intensity parts within high acoustic reflection intensity zones, and exposed rocks with thin sedimentary cover on slopes. Details of minute topographic changes which cannot be identified by MBES acoustic images were also clarified.

(Sampling)

Sampling by dredges and a corer was carried out at 128 sites in nine areas, MC02 to MC10. Manganese crusts were recovered from 105 sampling points, but samples from 69 points were sufficient in quantity for chemical analysis.

Chemical analysis, polished section microscopy, and ^{10}Be isotope analysis were carried out for the collected manganese crusts. And for rock samples, chemical analysis, thin section microscopy, X-ray diffractometry, K-Ar age determination, and fossil identification were carried out.

(Geology)

On seamounts in MC02 to MC06 areas, reef limestone occur from the summit to the upper slope to water depth of 1,600 ~ 2,000 m, and basalt and hyaloclastite are distributed in the lower slope. On those in the MC07 area, reef limestone occur in parts of the flat summit, but basalt and hyaloclastite dominantly occur from the summit to the lower slope. On those in areas MC08 to MC10, basalt and hyaloclastite occur from the summit to the lower slope and reef limestone does not occur. And on typical guyots of MC08 and MC10 areas, large amount of mudstone occur on the flat summit to the upper slope.

Chemical analysis of the basalts shows that; the basalt in MC02 area is a plume type mid-oceanic ridge basalt, that in MC04 area is island-arc tholeiite ~ normal mid-oceanic ridge basalt, and in MC05 and MC07 ~ MC10 areas it is classified as oceanic island alkali basalt.

(Seafloor observation)

Seafloor was observed by towed camera along nine track lines in six areas.

Generally on seamount slopes, crusts and cobble crusts are exposed intermittently on steep slopes while foraminifera sand covers the crusts on gentle slopes and the crusts are exposed in scattered pattern. Ripple marks occur on the surface of the foraminifera sand.

Crusts and cobble crusts are exposed continuously and nodules occur locally at the peripheries and small hills of the flat summits of the seamounts in MC07, MC08, and MC10 areas. Limestone without manganese oxide cover is distributed from the summit to about 800 m water depth in the seamounts in MC04 area.

(Thickness of manganese crusts)

The maximum, minimum, and average thickness of manganese crusts were measured at each sampling points and average crust thickness of each area was calculated. The crusts of MC02, MC08, and MC10 areas is relatively thick on at 20 ~ 21 mm on average. The average thickness of the crusts in MC03, MC04, MC06, MC07, and MC09 areas is thin, 1 ~ 8 mm, and that of MC05 area is very thin, under 1 mm.

Crusts with maximum thickness exceeding 50 mm were recovered from; one locality in MC02, five localities in MC08, and three localities in MC10 areas. The maximum in the three MC10 localities exceeded 100 mm.

(Chemical analysis of manganese crusts)

Twenty nine elements in 163 samples were chemically analyzed. These samples are from 113 manganese crusts from 69 localities. The average grades of Co, Ni, Cu, Mn, Fe are; 0.41, 0.32, 0.06, 24.12, 15.83 wt% respectively. The range of Co average grade is 0.33 ~ 0.36 % in MC02, MC08, and MC10, and that of other areas is 0.47 ~ 0.49 %, thus the difference by area is large and clear.

The results of factor analysis show that the major elements of the manganese crusts are expressed as one factor, and are divided into two groups by factor loading values. The groups are; Co, Ni, Mn, Pb, Mo, V, concentration and Cu, Fe, Si, Al, Ti concentration and there is negative correlation between the two groups.

(Mineral composition of manganese crusts)

Vernadite and todorokite were identified as the major minerals comprising manganese crusts of the present survey area. These minerals are very fine-grained and microcrystalline, and one of them tend to occur dominantly. The mode of occurrence differ by sample and the layer within the crust. Banded or kidney texture is developed in the black compact parts, and prismatic, granular, colloform texture in porous parts accompanied by brown oxides. The width of the growth bands is 5 ~ 50 μ m.

(Mode of occurrence of manganese crusts)

Manganese crusts with thickness over 10 mm occur in water depth range of 1,000 m to 3,500 m. Manganese crusts occur as crusts, cobbles, and nodules, and their thickness differs greatly by area, topography, substrate and other factors.

Thick manganese crusts exceeding 50 mm with average of about 20 mm were recovered in MC02, MC08, and MC10 areas. But the areal extent of manganese crust occurrence in MC02 is narrow. Manganese crusts in MC04 and MC05 areas are exposed well, but their thickness is very thin with an average of around 1 mm.

The average grades of the major constituent elements differ by area. In MC02, MC08, and MC10 areas, Cu content is higher than in other areas, but Co and Mn content is low. Mn content is the highest, but Fe is the lowest in MC04 area.

Based on the mode of occurrence of the manganese crusts, MC08 and MC10 areas are assessed as having the highest potential and other areas are considerably lower.

[REFERENCES]

Bonani G., Hofmann H.J., Morenzoni E., Nessi M., Suter M., and Wolfli W, 1984, ^{10}Be dating of the inner structure of Mn-encrustations applying the Zurich Tandem Accelerator, Nuclear Instruments and Methods in Physics Research B5, 359-364

Brevart O., B. Dupre and C.J. Allegre, 1981, Metallogenesis at spreading centers; lead isotope systematics for sulfides, manganese-rich crusts, basalts and sediments from Cyamax and Alvin areas (East Pacific Rise). Econ. Geol. Bull. Soc. Econ. Geologists., 76, 5, p. 1205-1210.

De Carlo E.R. and C.M. Fraley, 1992, Chemistry and mineralogy of ferromanganese deposits from the equatorial Pacific Ocean., Geology and offshore mineral resources of the central Pacific basin, p. 225-245.

Hart S., 1984, A large scale anomaly in the Southern Hemisphere mantle. Nature 309, 753-757.

Haynes B.W. and M.J. Magyar, 1987, Analysis and metallurgy of manganese nodules and crusts., Marine Minerals, p. 235-246.

Hein J.R., M.S. Schulz, and L.M. Gein, 1992, Central Pacific cobalt-rich ferromanganese crusts: Historical perspective and regional variability., Geology and offshore mineral resources of the central Pacific basin, p. 261-283.

Hein J.R., W.C. Schwab and A.S. Davis, 1988, Cobalt-and Platinum-rich ferromanganese crusts and associated substrate rocks from the Marshall islands., Marine Geology, v. 78, p. 255-283.

Hein J.R. et al., 1990, Geological, Geochemical, Geophysical, and Oceanographic Data and Interpretations of Seamounts and Co-rich Ferromanganese Crusts from the Marshall Islands, KORDIUSGS R.V. Farnella Cruise F10-89-CP.

Janney P.E. and P.R. Castillo, 1996, Basalts from the central Pacific basin: Evidence for the origin of Cretaceous igneous complexes in the Jurassic western Pacific., vol. 101, no. B2, p. 2875-2893.

JICA-MMAJ, 1997, Report on the cooperative study project on the deepsea mineral resources in selected offshore areas of the SOPAC region sea area of the Republic of the Marshall Islands, p. 180

Lincoln J., M.S. Prigle and I.P. Silva, 1993, Early and late Cretaceous volcanism and reef-building in the Marshall Island. in The Mesozoic Pacific; Geology, Tectonics, and Volcanism., Geophysical Monograph 77.

Mangini A., P. Halbach, D. Puteanus, and M. Segl, 1987, Chemistry and growth history of central Pacific Mn-crusts and their economic importance., Marine Minerals, p. 205-220.

Mullen E.D., 1983, $MnO/TiO_2/P_2O_5$: a minor element discriminant for basalt rocks of oceanic enviroments and its implications for petrogenesis. Earth Planet. Sci. Lett., 62, 53-62.

Sharma P. and B.L.K. Somauajulu, 1982, ^{10}Be dating of large manganese nodules from world oceans., Earth ahronology, Earth Planet. sci. Let., v.36, p. 359-362.

KORDI-USGS (Hein J.R. et al.), 1992, Geology, Geophysics, Geochemistry, and Deep-Sea Mineral Deposits, Federated States of Micronesia: R.V. Farnella Cruise F11-90-CP, USGS Open File Report 92-218.

Usui A., 1995, Studies of marine manganese deposits: Review and perspectives., Chishitsu News, no. 493, p. 30-41. (Japanese)

Verma S.P., 1992, Seawater alteration effects on REE, K, Rb, Cs, Sr, U, Th, Pb and Sr-Nd-Pb isotope systematics of Mid-ocean ridge basalt. Geochem. Jour., 36, 159-178.

Woodhead J.O. and C.W. Devey, 1993, Geochemistry of the Pitcairn seamounts, I: source character and temporal trends. Earth Planet. Sci. Left., 116, 81-99.

Zindler A. and S. Hart, 1986, Chemical geodynamics. Ann. REv. Earth Planet. Sci., 14, 493-571.

[APPENDIX]

Table 1	Results of FDC survey
Table 2(1)~(7)	Summary results of sampling
Table 3(1)~(4)	Results of chemical analysis for manganese crusts
Table 4(1)~(5)	Summary results of chemical analysis for manganese crusts
Table 5(1)~(4)	Sample list of analysis and observations
Table 6(1)~(3)	Sea-water sound velocity for MBES
Table 7	Weather and sea-state data
Fig. 1(1)~(10)	Location map of track line (area MC01 to MC10)
Fig. 2(1)~(10)	Color-coded bathymetric map based on MBES (area MC01 to MC10)
Fig. 3(2)~(10)	Topographic gradient map based on MBES (area MC02 to MC10)
Fig. 4(1)~(9)	Route map of FDC observation and exposed rate diagram of manganese crusts (area MC03 to MC04, MC07~MC10)

Appendix Table 1 Results of FDC survey

District	Track Line No.	Item	Date & Time (UTC)		FDC Position Latitude (N)	FDC Position Longitude (E)	Depth (m)	General Location	Observation Time	Observation Length	No. of Photos	No. of VTR Tapes
MC03	97SMC03FDC010	I S	Jul 28	21:59					3h 46m	3.8 nm	135	2
		SP		22:29	6° 17.693′	141° 32.693′	980	summit of west part of seamount				
		EP	Jul 29	2:15	6° 20.146′	141° 30.475′	2,751	middle part of northwest flank				
		OD		3:10								
	97SMC03FDC011	I S	Jul 29	3:56					2h 11m	1.9 nm	116	2
		SP		4:47	6° 19.390′	141° 29.407′	2,640	middle part of northwest flank				
		EP	Jul 29	6:58	6° 20.991′	141° 28.420′	3,870	lower part of northwest flank				
		OD		8:12								
MC04	97SMC04FDC01	I S	Aug 4	23:17					3h 45m	3.8 nm	152	2
		SP		23:54	6° 11.849′	144° 19.780′	1,860	upper part of southwest flank				
		EP	Aug 5	3:39	6° 09.211′	144° 17.058′	3,636	lower part of southwest flank				
		OD		4:50								
	97SMC04FDC02	I S	Aug 5	22:41					4h 32m	5.0 nm	255	3
		SP		22:48	6° 15.435′	144° 21.154′	178	summit				
		EP	Aug 6	3:20	6° 12.536′	144° 17.054′	2,669	middle part of southwest flank				
		OD		4:12								
MC07	97SMC07FDC01	I S	Aug 27	21:02					6h 03m	6.3 nm	265	4
		SP		21:39	6° 01.590′	157° 25.459′	1,569	summit part				
		EP	Aug 28	3:42	6° 03.582′	157° 19.537′	2,940	middle part of northwest flank				
		OD		4:41								
MC08	97SMC08FDC01	I S	Sep 2	21:15					2h 43m	2.4 nm	105	2
		SP		21:57	10° 21.597′	156° 44.650′	2,012	east margin of flat summit				
		EP	Sep 3	0:40	10° 23.582′	156° 46.074′	3,165	middle part of east flank				
		OD		1:40								
	97SMC08FDC02	I S	Sep 3	2:28					2h 02m	2.1 nm	117	2
		SP		3:09	10° 25.612′	156° 40.269′	1,969	north margin of flat summit				
		EP	Sep 3	5:11	10° 27.591′	156° 40.826′	2,284	north margin of flat summit				
		OD		5:59								
MC09	97SMC09FDC01	I S	Sep 12	21:50					2h 28m	2.3 nm	125	2
		SP		22:19	8° 05.198′	154° 58.894′	1,202	summit of southern seamount				
		EP	Sep 13	0:47	8° 03.732′	154° 57.059′	2,734	middle part of south flank				
		OD		5:59								
MC10	97SMC10FDC01	I S	Sep 20	21:40					4h 58m	4.8 nm	176	3
		SP		22:18	9° 55.075′	148° 14.138′	1,948	northeast margin of flat summit				
		EP	Sep 21	3:16	9° 56.751′	148° 09.587′	3,525	lower part of northeast flank				
		OD		4:22								

Legend I S: FDC into the sea, SP: Start point of observation, EP: End point of observation, OD: FDC on the deck.
Note FDC Position is calculated by GPS ship position, CTD depth of FDC and wire length.

Appendix Table 2 (1) Summary results of sampling

Site No.	Location Latitude (N)	Longitude (E)	Depth (m)	Topographic location	Crust type (LC photo contents)	Crust surface tex.	Crust thickness(mm) Max.	Min.	Ave.	Sample wt. (kg)	Substrate rocks / Unconsolidated sediments [core length / bit deformation]
MC02 district							(50)		(21)		
LC01	9° 14.967′	141° 35.009′	3,256	southeastern foot	not exist	-	-	-	-	35.6	foraminiferal ooze [215cm / unseen]
AD02	9° 08.457′	141° 37.456′	1,933	lower north flank to	no crusts recovered	-	-	-	-	0	no rocks recovered
	9° 08.255′	141° 36.557′	1,370	north summit margin							
CB03	9° 10.162′	141° 32.235′	3,335	lower north flank	stain	-	< 1	< 1	< 1	81.2	basalt (pillow lava), pyroclastic rock,
	9° 09.930′	141° 32.120′	3,320								altered basalt (pyrite disseminated)
CB04	8° 58.209′	141° 38.744′	1,558	southeast summit	crust	botryoidal	50	< 1	30	58.7	reefal limestone, foraminiferal sandstone,
	8° 58.049′	141° 38.538′	1,268	(pinnacle)	thin coating	smooth					porphyritic basalt pebble
LC05	8° 58.602′	141° 38.423′	1,636	ditto	crust	granular	35	30	32	0.19	no substrate rocks recovered
LC06	8° 58.516′	141° 33.921′	1,482	ditto	crust	botryoidal	25	20	22	1.08	phosphatized limestone
LC07	9° 07.601′	141° 41.942′	1,412	north summit margin	not exist	-	-	-	-	1.9	foraminiferal sand [23cm / unseen]
MC03 district							(47)		(8)		
LC01	6° 13.953′	141° 51.982′	3,508	southeastern foot	not exist	-	-	-	-	44.6	ooze, foraminiferal sand, ash [260cm / unseen]
AD02	6° 21.627′	141° 53.496′	2,105	upper southeast flank	crust	botryoidal	14	3	10	1.7	vesicular aphyric basalt,
	6° 21.628′	141° 53.527′	2,028			granular					pumice pebble
AD03	6° 20.593′	141° 51.293′	1,794	southeast summit margin	no crusts recovered	-	-	-	-	0.13	no rocks recovered
	6° 20.736′	141° 51.085′	1,756								
AD04	6° 21.775′	141° 47.687′	1,826	eastern summit center	crust	botryoidal	13	2	10	1.78	vesicular porphyritic basalt,
	6° 21.866′	141° 47.651′	1,777			~ granular					pumice pebble
AD05	6° 20.033′	141° 41.889′	1,542	summit center	cobble crust	botryoidal	10	< 1	1	45.61	reefal limestone, foraminiferal sandstone,
	6° 20.198′	141° 41.415′	1,466	(pinnacle)	thin coating	~ smooth					pumice pebble
CB06	6° 16.237′	141° 32.174′	1,177	western summit	cobble crust, nodule	botryoidal	10	< 1	< 1	221.2	reefal limestone, phosphatized limestone,
	6° 16.327′	141° 31.577′	1,109		thin coating	~ smooth					pebbly limestone
CB07	6° 21.791′	141° 34.019′	2,429	upper northwest flank	crust	botryoidal	15	< 1	5	1.34	vesicular aphyric basalt, pebbly foraminiferal
	6° 21.481′	141° 33.621′	2,247		thin coating	~ granular					sandstone, pumice pebble
CB08	6° 23.723′	141° 36.971′	2,907	middle northwest flank	crust	granular	15	10	12	1.57	no substrate rocks recovered,
	6° 23.530′	141° 36.644′	2,645								glassy vesicular basalt pebble, pumice pebble
CB09	6° 25.080′	141° 54.190′	1,179	upper northeast flank	crust, cobble crust	botryoidal	8	< 1	1	47.62	vesicular porphyritic basalt, hyaloclastite,
	6° 25.044′	141° 53.929′	1,079	(pinnacle)	thin coating	~ smooth					reefal limestone
CB10	6° 25.778′	141° 52.221′	2,137	middle northeast flank	cobble crust	botryoidal	6	< 1	< 1	26.5	porphyritic basalt, vesicular porphyritic basalt,
	6° 25.699′	141° 52.053′	1,996		thin coating	~ smooth					basalt conglomerate
CB11	6° 20.229′	141° 49.128′	1,832	southeast summit margin	crust	botryoidal	47	7	27	9.29	vesicular basalt,
	6° 20.261′	141° 49.126′	1,783			~ granular					foraminiferal sandstone, pumice pebble
CB12	6° 18.087′	141° 46.812′	2,046	upper south flank	crust	granular	25	20	20	1.74	no substrate rocks recovered,
	6° 18.234′	141° 46.368′	2,093								pumice pebble
CB13	6° 26.160′	141° 45.814′	2,873	lower north flank	crust	granular	15	< 1	4	3.12	vesicular porphyritic basalt, porphyritic basalt,
	6° 26.962′	141° 45.514′	2,671								pumice pebble

Appendix Table 2 (2) Summary results of sampling

Site No.	Location Latitude (N)	Location Longitude (E)	Depth (m)	Topographic location	Crust type (LC photo contents)	Crust surface tex.	Crust thickness(mm) Max.	Crust thickness(mm) Min.	Crust thickness(mm) Ave.	Sample wt. (kg)	Substrate rocks / Unconsolidated sediments [core length / bit deformation]
LC14	6° 29.220′	141° 42.800′	2,904	northern foot (ridge)	not exist	-	-	-	-	0.07	weekly consolidated foraminiferal sand [7cm /unseen]
LC15	6° 22.406′	141° 37.725′	* 2,096	north summit margin	(crust)	(granular)	5	5	5	0.024	basalt
LC16	6° 15.017′	141° 34.128′	1,979	upper south flank	(cobble crust)	(granular)	-	-	-	0	nothing recovered
MC04 district				(MC04 has two seamounts)			(20)		(1)		
LC01	6° 01.531′	144° 29.024′	3,876	southeast foot of the west	not exist	-	-	-	-	24.8	foraminiferal sand, limestone pebble [160cm /unseen]
CB02	6° 19.762′	144° 19.428′	2,193	western seamount	no crusts recovered	-	-	-	-	0.571	no substrate rocks recovered,
	6° 19.388′	144° 19.805′	1,959	middle north flank							foraminiferal sand, pumice pebble
CB03	6° 18.059′	144° 18.313′	1,887	western seamount	thin coating	smooth	<1	<1	<1	6.13	reefal limestone,
	6° 17.454′	144° 18.419′	1,703	middle north flank	stain						pumice pebble
CB04	6° 13.558′	144° 19.849′	* 1,305	western seamount	thin coating	smooth	<1	<1	<1	4.833	reefal limestone, foraminiferal limestone,
	6° 13.697′	144° 19.118′	* 1,303	upper southwest flank	stain						pumice pebble
CB05	6° 11.660′	144° 19.711′	* 1,944	western seamount	thin coating	smooth	<1	<1	<1	10.1	reefal limestone,
	6° 11.992′	144° 19.352′	* 1,972	middle southwest flank							pumice pebble
CB06	6° 17.733′	144° 25.641′	1,303	western seamount	thin coating	smooth	<1	<1	<1	49.752	reefal limestone,
	6° 17.952′	144° 25.335′	1,153	east summit (ridge)							vesicular glassy basalt pebble
CB07	6° 15.497′	144° 28.302′	2,461	western seamount	thin coating	smooth	2	<1	<1	9.131	vesicular porphyritic basalt (pillow breccia),
	6° 15.134′	144° 27.884′	2,258	lower east flank							reefal limestone, pumice pebble
CB08	6° 12.671′	144° 25.429′	2,532	western seamount	thin coating	smooth	1	<1	<1	29.086	vesicular porphyritic basalt (pillow breccia),
	6° 12.618′	144° 25.368′	2,245	lower southeast flank							reefal limestone, pumice pebble
CB09	6° 10.992′	144° 24.160′	2,434	western seamount	thin coating	smooth	<1	<1	<1	0.582	vesicular porphyritic basalt, limestone,
	6° 10.774′	144° 23.802′	2,246	lower southeast flank							pumice pebble
CB10	6° 07.792′	144° 45.736′	1,454	eastern seamount	cobble crust, nodule	botryoidal	6	<1	3	116.21	reefal limestone,
	6° 08.210′	144° 45.355′	1,452	summit center	thin coating	~ smooth					pumice pebble
CB11	6° 09.569′	144° 45.549′	1,928	eastern seamount	crust, cobble crust,	botryoidal	5	<1	1	10.04	reefal limestone, porous limestone,
	6° 10.045′	144° 45.143′	1,680	upper northeast flank	nodule, thin coating	~ smooth					mudstone (subrounded pebble)
CB12	6° 10.021′	144° 39.789′	2,008	eastern seamount	crust, nodule	botryoidal	3	<1	1	1.366	vesicular aphyric basalt, pyroclastic rock,
	6° 10.461′	144° 39.354′	1,746	middle west flank	thin coating	~ granular					foraminiferal limestone, pumice pebble
CB13	6° 12.456′	144° 39.461′	2,365	eastern seamount	crust	botryoidal	20	8	10	2.75	no substrate rocks recovered,
	6° 12.368′	144° 39.312′	2,194	middle northwest flank		~ granular					foraminiferal limestone, pumice pebble
CB14	6° 21.305′	144° 30.250′	836	east to western seamount	crust ~ thin coating	granular ~	2	<1	<1	2.16	foraminiferal limestone
	6° 21.251′	144° 30.130′	687	summit of ridge		smooth					
CB15	6° 15.183′	144° 21.411′	485	western seamount	stain	smooth	<1	<1	<1	7.71	reefal limestone
	6° 15.078′	144° 21.134′	301	upper south flank							
CB16	6° 16.136′	144° 18.059′	1,173	western seamount	thin coating	smooth	1	<1	<1	3.06	foraminiferal limestone
	6° 16.025′	144° 17.937′	832	upper north flank							
CB17	6° 14.897′	144° 14.252′	1,817	western seamount	crust	botryoidal	15	5	10	1.73	vesicular basalt,
	6° 15.034′	144° 13.853′	1,463	upper southwest flank		~ granular					pumice pebble

Appendix Table 2 (3) Summary results of sampling

Site No.	Location Latitude (N)	Longitude (E)	Depth (m)	Topographic location	Crust type (LC photo contents)	Crust surface tex.	Crust thickness(mm) Max.	Min.	Ave.	Sample wt. (kg)	Substrate rocks / Unconsolidated sediments [core length / bit deformation]
CB18	6° 06.451′	144° 48.852′	2,651	eastern seamount	crust	granular	11	<1	<1	17.773	vesicular basalt, porphyritic basalt,
	6° 06.727′	144° 48.585′	2,432	lower east flank	thin coating ~ stain	smooth					hyaloclastite, reefal limestone
CB19	6° 13.298′	144° 46.009′	1,699	eastern seamount	crust	botryoidal	3	<1	<1	2.93	reefal limestone
	6° 13.298′	144° 45.809′	1,513	upper northeast flank	thin coating ~ stain	smooth					
LC20	6° 15.375′	144° 50.613′	2,408	northeast foot of the east	not exist	-	-	-	-	22.4	foraminiferal sand [150cm / unseen]
LC21	6° 14.398′	144° 53.187′	2,198	northeast foot of the east	(crust ?)	(smooth)	-	-	-	0	nothing recovered
MC05 district							(<1)		(<1)		
LC01	5° 25.939′	149° 32.029′	4,060	southeastern foot	not exist	-	-	-	-	49.7	foraminiferal ~ calcareous ooze [280cm / unseen]
CB02	5° 38.198′	149° 15.837′	3,048	lower northeast flank	stain	-	<1	<1	<1	13.654	vesicular basalt (pillow breccia), limestone,
	5° 38.086′	149° 15.783′	2,823								pumice pebble
CB03	5° 36.754′	149° 13.815′	2,388	middle northeast flank	stain	-	<1	<1	<1	5.14	vesicular porphyritic basalt, aphyric basalt,
	5° 36.533′	149° 13.655′	2,197								hyaloclastite, conglomerate, sandstone, limestone
CB04	5° 34.129′	149° 13.201′	1,417	upper northeast flank	stain	-	<1	<1	<1	8.335	reefal limestone
	5° 33.824′	149° 13.041′	1,082								
CB05	5° 32.636′	149° 16.788′	2,017	middle northeast flank	thin coating	smooth	<1	<1	<1	2.58	conglomerate, aphyric basalt, limestone,
	5° 32.330′	149° 16.550′	1,784		stain						pumice pebble
CB06	5° 25.014′	149° 15.008′	2,157	middle southeast flank	thin coating	smooth	<1	<1	<1	1.906	basaltic pyroclastic rock, porphyritic glassy basalt,
	5° 24.777′	149° 14.827′	1,829		stain						reefal limestone, pumice pebble
CB07	5° 26.094′	149° 14.096′	1,500	upper southeast flank	thin coating	smooth	<1	<1	<1	28.48	reefal limestone,
	5° 25.865′	149° 13.545′	1,204								pumice pebble
CB08	5° 27.621′	149° 09.405′	2,008	middle south flank	thin coating	smooth	<1	<1	<1	2.96	limestone,
	5° 27.466′	149° 09.268′	1,714		stain						pumice pebble
CB09	5° 26.697′	149° 03.110′	2,644	middle south flank	no crusts recovered	-	-	-	-	0.299	aphyric basalt, limestone,
	5° 26.390′	149° 02.814′	2,363								pumice pebble
MC06 district							(20)		(3)		
CB01	4° 24.409′	147° 51.021′	2,605	lower north flank	stain	-	<1	<1	<1	0.402	porphyritic basalt, limestone,
	4° 24.249′	147° 50.853′	2,190								
CB02	4° 22.223′	147° 54.129′	2,054	middle northeast flank	crust	botryoidal	10	3	4	33.643	vesicular porphyritic ~ aphyric basalt,
	4° 21.936′	147° 53.873′	1,751			~ granular					hyaloclastite, tuff, pumice pebble
CB03	4° 19.342′	147° 52.712′	1,932	middle south flank	stain	-	<1	<1	<1	1.06	limestone,
	4° 19.403′	147° 52.155′	1,828								pumice pebble
CB04	4° 22.299′	147° 48.250′	1,969	middle northwest flank	crust	granular	20	<1	5	2.05	foraminiferal limestone
	4° 21.976′	147° 47.991′	1,795		thin coating						pumice pebble
CB05	4° 26.426′	147° 59.263′	2,636	lower north flank	crust	granular	3	1	2	1.788	vesicular porphyritic basalt, hyaloclastite,
	4° 26.224′	147° 58.998′	2,358		stain						reefal limestone, foraminiferal limestone, pumice
CB06	4° 22.256′	147° 57.529′	1,937	summit center (ridge)	crust, cobble crust,	botryoidal	13	1	4	114.7	hyaloclastite, conglomerate,
	4° 22.147′	147° 57.176′	1,840		nodule	~ granular					reefal limestone

Appendix Table 2 (4) Summary results of sampling

Site No.	Location Latitude (N)	Location Longitude (E)	Depth (m)	Topographic location	Crust type (LC photo contents)	Crust surface tex.	Crust thickness (mm) Max.	Crust thickness (mm) Min.	Crust thickness (mm) Ave.	Sample wt. (kg)	Substrate rocks / Unconsolidated sediments [core length / bit deformation]
CB07	4° 23.681′	148° 01.722′	1,681	summit center (ridge)	crust	botryoidal	7	< 1	< 1	64.7	reefal limestone
	4° 23.519′	148° 01.637′	1,516		thin coating ~ stain	~ granular					
CB08	4° 26.097′	148° 05.810′	1,625	upper north flank	crust, cobble crust	botryoidal	12	< 1	4	64.41	reefal limestone
	4° 25.845′	148° 05.561′	1,421		thin coating	granular					
MC07 district							(14)		(5)		
LC01	6° 07.862′	157° 17.968′	3,079	western foot	not exist	-	-	-	-		foraminiferal sand [145cm / unseen]
CB02	6° 03.074′	157° 30.993′	2,609	middle east flank	crust	botryoidal	14	2	7	6.019	vesicular porphyritic basalt (pillow lava),
	6° 03.021′	157° 30.560′	2,129			~ granular					pumice pebble
CB03	6° 04.587′	157° 31.092′	2,941	middle east flank	crust	granular	11	7	9	0.38	no substrate rocks recovered,
	6° 04.560′	157° 30.693′	2,716			~ smooth					pumice pebble
CB04	6° 06.125′	157° 30.118′	2,610	middle east flank	crust	granular	6	3	5	1.24	vesicular porphyritic basalt
	6° 06.120′	157° 29.884′	2,379								
CB05	6° 08.278′	157° 29.474′	2,256	upper east flank	crust	botryoidal	8	< 1	3	6.929	hyaloclastite, vesicular basalt,
	6° 08.200′	157° 29.008′	2,203		thin coating	~ granular					sandstone, mudstone, foraminiferal sandstone
AD06	5° 59.594′	157° 24.209′	1,671	summit center (pinnacle)	crust, cobble crust	botryoidal	10	1	4	3.417	vesicular porphyritic ~ aphyric basalt,
	5° 59.550′	157° 24.091′	1,446			~ granular					limestone
AD07	6° 02.836′	157° 20.436′	2,637	middle west flank	thin coating	smooth	< 1	< 1	< 1	0.98	porphyritic basalt (pillow lava)
	6° 02.460′	157° 20.166′	2,640								
AD08	6° 05.606′	157° 20.650′	2,614	middle west flank	crust	granular	7	1	5	1.74	vesicular aphyric basalt,
	6° 05.833′	157° 20.548′	2,480								calcareous sandstone, pumice pebble
AD09	6° 05.987′	157° 22.413′	2,027	upper west flank	crust	botryoidal	12	4	8	3.46	hyaloclastite,
	6° 05.747′	157° 22.151′	2,039			~ granular					pumice pebble
LC10	6° 03.490′	157° 19.587′	2,928	middle west flank	(crust ?)	-	-	-	-	0	nothing recovered
LC11	6° 02.008′	157° 20.729′	2,372	upper west flank (terrace)	not exist	-	-	-	-	29.1	foraminiferal sand [200cm / unseen]
LC12	6° 02.651′	157° 23.085′	2,041	west summit margin	(not exist)	-	-	-	-	0.009	basalt fragment [/ seen]
LC13	5° 57.527′	157° 23.714′	1,472	summit center (pinnacle)	(crust)	(granular)	-	-	-	0	nothing recovered
CB14	6° 12.432′	157° 29.106′	2,889	middle northeast flank	crust	granular	8	< 1	1	1.424	basaltic tuff breccia,
	6° 12.351′	157° 29.062′	2,689								pumice pebble
CB15	5° 59.206′	157° 28.024′	1,952	southeast summit margin	cobble crust, nodule	botryoidal	7	< 1	2	16.148	hyaloclastite, vesicular porphyritic basalt,
	5° 58.978′	157° 27.787′	1,657	(pinnacle)		~ smooth					pumice pebble
MC08 district							(90)		(20)		
LC01	10° 19.986′	156° 26.940′	5,208	western foot	crust	smooth	15	6	10	2	calcareous mud ~ sand, ooze [20cm / unseen]
CB02	10° 28.429′	156° 40.858′	2,916	upper north flank	crust, cobble crust	granular ~	70	< 1	50	24.95	vesicular aphyric basalt, porphyritic basalt,
	10° 28.631′	156° 41.132′	2,697			botryoidal					conglomerate, limestone
CB03	10° 26.491′	156° 38.678′	3,010	upper northwest flank	crust, cobble crust	granular	10	< 1	2	4.311	porphyritic basalt, conglomerate,
	10° 26.561′	156° 39.236′	2,832								pumice pebble

Appendix Table 2 (5) Summary results of sampling

Site No.	Location Latitude (N)	Longitude (E)	Depth (m)	Topographic location	Crust type (LC photo contents)	Crust surface tex.	Crust thickness(mm) Max.	Min.	Ave.	Sample wt. (kg)	Substrate rocks / Unconsolidated sediments [core length / bit deformation]
CB04	10° 26.425′	156° 40.487′	2,177	north summit margin	crust, cobble crust,	botryoidal	25	< 1	6	35.082	mudstone, hyaloclastite, limestone,
	10° 26.538′	156° 40.839′	2,157		nodule	~ smooth					pumice pebble
CB05	10° 24.078′	156° 40.802′	1,836	northwest summit margin	cobble crust, nodule	botryoidal	90	10	45	201.8	hyaloclastite
	10° 24.475′	156° 40.378′	1,682	(pinnacle)		granular					
CB06	10° 21.893′	156° 36.782′	2,251	west summit margin	crust	botryoidal	26	< 1	5	4.03	mudstone, hyaloclastite
	10° 22.211′	156° 37.095′	2,206		nodule	~ granular					
CB07	10° 21.703′	156° 35.398′	2,846	middle west flank	crust, cobble crust,	granular ~	11	< 1	1	169.3	spherulitic aphyric basalt,
	10° 22.063′	156° 35.638′	2,616		nodule	smooth					hyaloclastite, limestone
CB08	10° 19.902′	156° 37.283′	2,380	upper west flank	crust, cobble crust,	botryoidal	83	8	43	21.53	mudstone
	10° 20.077′	156° 37.617′	2,224		nodule	granular					
CB09	10° 17.572′	156° 39.319′	2,583	upper southwest flank	crust	botryoidal	40	10	27	3.48	vesicular glassy basalt, hyaloclastite,
	10° 17.732′	156° 39.860′	2,179			~ granular					pumice pebble
CB10	10° 17.645′	156° 40.184′	1,994	south summit margin	crust	botryoidal	30	1	15	1.688	vesicular aphyric basalt, hyaloclastite,
	10° 17.740′	156° 40.674′	1,807	(pinnacle)	nodule	granular					phosphorite, pumice pebble
CB11	10° 16.576′	156° 42.332′	2,342	upper south flank	crust	granular ~	15	< 1	7	1.667	phosphorite
	10° 16.964′	156° 42.638′	2,115		thin coating	smooth					
CB12	10° 17.705′	156° 45.208′	2,598	upper southeast flank	crust, cobble crust,	botryoidal	45	< 1	12	10.169	porphyritic basalt, vesicular porphyritic basalt,
	10° 18.137′	156° 45.516′	2,483		nodule	granular					hyaloclastite, conglomerate, phosphorite, mudstone
CB13	10° 24.804′	156° 34.729′	3,574	lower northwest flank	crust	granular ~	24	< 1	13	8.095	hyaloclastite, porphyritic basalt,
	10° 24.409′	156° 35.092′	3,202		thin coating	smooth					mudstone, pumice pebble
CB14	10° 25.575′	156° 40.226′	2,075	northwest summit margin	crust, nodule	granular	70	< 1	28	10.28	vesicular aphyric basalt, hyaloclastite
	10° 25.581′	156° 40.410′	1,851	(pinnacle)		smooth					
CB15	10° 22.410′	156° 45.223′	2,409	upper east flank	crust	granular	36	14	30	0.594	porphyritic basalt, conglomerate
	10° 22.066′	156° 45.341′	2,362								
LC16	10° 23.984′	156° 38.650′	2,129	northwest summit margin	crust	botryoidal	70	60	65	0.96	vesicular porphyritic basalt,
LC17	10° 26.431′	156° 40.458′	2,156	north summit margin	(nodule, sand)	-	-	-	-	0	nothing recovered [/ seen]
CB18	10° 26.895′	156° 34.772′	4,318	lower northwest flank	thin coating	smooth	< 1	< 1	< 1	42.31	spherulitic aphyric basalt, vesicular porphyritic
	10° 26.601′	156° 35.669′	4,055								basalt, phosphorite, pumice pebble
CB19	10° 20.357′	156° 34.315′	3,240	lower west flank	crust, cobble crust,	botryoidal	27	1	5	54.23	aphyric basalt, vesicular porphyritic basalt,
	10° 20.878′	156° 34.864′	2,930		nodule	granular					hyaloclastite, limestone
MC09 district				(MC09 has two seamounts)			(23)		(7)		
LC01	8° 13.786′	154° 57.379′	4,758	northern foot of the south	thin coating	smooth	< 1	< 1	< 1	2.7	ooze, phosphatized sand [40cm / unseen]
CB02	8° 06.521′	154° 57.849′	2,253	southern seamount	crust	granular	12	6	8	3.692	vesicular porphyritic basalt, vesicular aphyric
	8° 06.485′	154° 57.560′	1,975	middle north flank	thin coating						basalt, conglomerate
CB03	8° 05.771′	154° 58.790′	1,370	southern seamount	crust	botryoidal	12	1	8	80.65	vesicular aphyric basalt, basalt volcanic breccia
	8° 05.660′	154° 58.665′	1,122	upper east flank	thin coating						

Appendix Table 2 (6) Summary results of sampling

Site No.	Location Latitude (N)	Location Longitude (E)	Depth (m)	Topographic location	Crust type (LC photo contents)	Crust surface tex.	Crust thickness(mm) Max.	Min.	Ave.	Sample wt. (kg)	Substrate rocks / Unconsolidated sediments [core length / bit deformation]
CB04	8° 04.010′	154° 59.026′	2,401	southern seamount	crust	granular	10	5	8	1.393	vesicular basalt
	8° 04.125′	154° 58.952′	2,240	middle south flank							pumice pebble
CB05	8° 04.985′	155° 00.633′	2,647	southern seamount	crust ~ thin coating	granular	2	< 1	< 1	1.521	hyaloclastite
	8° 04.931′	155° 00.385′	2,395	middle east flank							
CB06	8° 08.760′	154° 57.703′	3,470	southern seamount	crust	granular ~	23	1	13	19.37	vesicular porphyritic basalt, vesicular aphyric
	8° 08.785′	154° 57.369′	3,253	lower north flank	thin coating	smooth					basalt, hyaloclastite, conglomerate
CB07	8° 06.395′	154° 53.760′	2,647	southern seamount	crust, cobble crust,	granular	14	1	9	23.005	vesicular aphyric basalt, basalt tuff breccia
	8° 06.197′	154° 53.522′	2,408	middle northeast flank	nodule						
CB08	8° 23.613′	155° 12.112′	3,016	northern seamount	crust, cobble crust,	botryoidal	14	1	7	48.273	vesicular porphyritic basalt
	8° 23.869′	155° 11.750′	2,699	northeast pinnacle summit	nodule	~ granular					
CB09	8° 20.917′	155° 11.075′	3,487	northern seamount	crust	granular	11	< 1	5	4.6	vesicular glassy aphyric basalt, conglomerate
	8° 20.900′	155° 10.874′	3,231	middle southeast flank							
CB10	8° 21.123′	155° 07.095′	2,349	northern seamount	crust	granular	11	2	7	2.6	vesicular porphyritic basalt
	8° 21.045′	155° 07.106′	2,182	center summit							
CB11	8° 23.304′	155° 05.571′	2,666	northern seamount	crust, cobble crust	granular	13	1	8	11.549	vesicular porphyritic basalt
	8° 23.244′	155° 05.470′	2,546	north ridge of center summit							
CB12	8° 24.524′	155° 05.188′	2,716	northern seamount	crust, cobble crust,	botryoidal	15	1	9	5.974	vesicular porphyritic basalt
	8° 24.433′	155° 05.001′	2,537	northwest pinnacle summit	nodule	~ granular					
CB13	8° 27.057′	155° 08.273′	2,979	northern seamount	crust, cobble crust	granular ~	12	1	8	23.496	vesicular porphyritic basalt
	8° 26.818′	155° 07.909′	2,709	north pinnacle summit		smooth					
MC10 district							(155)		(20)		
LC01	9° 51.343′	148° 40.666′	4,366	eastern foot	(nodule)	-	-	-	-	12.8	sandy ooze, granule, ooze [90cm / unseen]
CB02	9° 48.407′	148° 30.642′	2,086	upper east flank	crust, cobble crust	botryoidal	33	< 1	7	41.33	porphyritic basalt, conglomerate
	9° 48.269′	148° 30.326′	1,789			~ granular					
CB03	9° 49.986′	148° 27.989′	1,809	northeast summit margin	crust	botryoidal	12	8	10	0.43	no substrate rocks recovered
	9° 49.863′	148° 27.710′	1,775			granular					pumice pebble
CB04	9° 52.708′	148° 05.803′	2,587	middle northwest flank	crust	botryoidal	120	10	30	12.3	vesicular porphyritic basalt, hyaloclastite,
	9° 52.537′	148° 05.791′	2,527			granular					conglomerate, consolidated foraminiferal sand
CB05	9° 54.441′	148° 11.247′	1,902	north summit margin	crust, cobble crust,	botryoidal	24	2	10	2.63	mudstone
	9° 54.145′	148° 10.759′	1,872		nodule	granular					pumice pebble
CB06	9° 55.938′	148° 14.067′	2,038	upper north flank	crust, nodule	botryoidal	107	10	90	16.9	no substrate rocks recovered
	9° 55.590′	148° 13.804′	1,927			granular					
CB07	9° 57.924′	148° 16.157′	*2,262	upper north flank	crust, cobble crust	granular	155	5	109	38.54	hyaloclastite, mudstone
	9° 57.535′	148° 15.885′	*2,186	(pinnacle on the terrace)	thin coating						
CB08	9° 54.132′	148° 30.656′	*3,240	lower northeast flank	no crusts recovered	-	-	-	-	0	nothing recovered
	9° 54.077′	148° 30.449′	*3,124								

Appendix Table 2 (7) Summary results of sampling

Site No.	Location Latitude (N)	Location Longitude (E)	Depth (m)	Topographic location	Crust type (LC photo contents)	Crust surface tex.	Crust thickness(mm) Max.	Crust thickness(mm) Min.	Crust thickness(mm) Ave.	Sample wt. (kg)	Substrate rocks / Unconsolidated sediments [core length / bit deformation]
CB09	9° 52.129′	148° 28.826′	*2,756	middle northeast flank	nodule	smooth	9	<1	<1	15.528	porphyritic basalt, hyaloclastite, mudstone,
	9° 51.579′	148° 28.533′	*2,595		thin coating						phosphorite, pumice pebble
CB10	9° 35.729′	148° 23.872′	*2,810	middle southeast flank	crust	granular	10	<1	<1	3.032	porphyritic basalt, conglomerate, phosphorite
	9° 35.582′	148° 23.312′	*2,755		thin coating						pumice pebble
CB11	9° 37.306′	148° 23.975′	*2,322	upper southeast flank	crust, cobble crust	granular	12	<1	3	2.97	porphyritic basalt, conglomerate
	9° 37.280′	148° 23.568′	*2,126								
CB12	9° 40.419′	148° 27.089′	*2,152	southeast summit margin	nodule	botryoidal	15	1	3	9.05	mudstone, porphyritic basalt
	9° 40.234′	148° 26.612′	*2,050			~ granular					pumice pebble
CB13	9° 35.769′	148° 15.460′	*2,414	upper south flank	nodule	granular	5	<1	<1	1.46	vesicular porphyritic basalt, conglomerate,
	9° 35.739′	148° 15.132′	*2,325		thin coating						phosphorite
CB14	9° 36.481′	148° 13.014′	*1,741	south summit margin	crust	botryoidal	15	<1	5	0.516	vesicular porphyritic basalt, conglomerate
	9° 36.339′	148° 12.719′	*1,593	(pinnacle)		~ granular					
CB15	9° 35.206′	148° 10.733′	*2,727	middle south flank	crust, nodule	botryoidal	35	5	22	0.975	vesicular porphyritic basalt
	9° 35.360′	148° 10.425′	*2,751			~ granular					
CB16	9° 37.560′	148° 11.416′	*1,931	southwest summit margin	crust, cobble crust	botryoidal	12	<1	2	1.99	mudstone, phosphatized ooze
	9° 38.021′	148° 10.892′	*1,986			~ smooth					pumice pebble
LC17	9° 54.228′	148° 11.218′	1,952	north summit margin	(not exist)	-	-	-	-	0	nothing recovered [/ seen]
LC18	9° 55.286′	148° 13.873′	1,928	north summit margin	not exist	-	-	-	-	3.2	foraminiferal sand [30cm / seen]
CB19	9° 56.750′	148° 12.505′	*2,296	upper north flank	crust, nodule	botryoidal	30	2	13	9.81	hyaloclastite, vesicular porphyritic basalt,
	9° 56.310′	148° 12.006′	*2.287			~ granular					mudstone, pumice pebble
CB20	9° 54.269′	148° 22.155′	*2,356	upper north flank	crust, cobble crust,	botryoidal	21	<1	8	40.699	aphyric ~ porphyritic basalt, vesicular aphyric
	9° 53.875′	148° 21.860′	*2,212		nodule	~ granular					basalt, conglomerate, mudstone, pumice pebble

note: Location shows the GPS location of the ship.
Water depth is based on the TD or CTD measurements, but the value with an asterisk shows MBES water depth of the ship location.
Dredge sampling (station No. includes AD or CB) data is composed of two lines.
The upper line of location and water depth columns means the data when the dredger touched down the seafloor, and the lower line when it left from.
Values in parentheses on the column of crust thickness mean the maximum thickness and the average thickness in the district.